ministerie van verkeer en waterstaat

rijkswaterstaat

dienst getijdewateren

nota GWAO-87.022

Eddy simulation of two-dimensional dispersion

G.C. van Dam

Den Haag December 1987 The Hague

Samenvatting

Deze nota beschrijft een onderzoek betreffende het gedrag van deeltjes-wolken in tweedimensionale snelheidsvelden. De resultaten kunnen in ruime zin geïnterpreteerd worden, maar zijn in het bijzonder van belang voor de verspreiding van stoffen in oppervlaktewateren van grote horizontale uitgebreidheid en een in verhouding geringe diepte of laagdikte. De relevantie voor de zee is wellicht wat groter dan voor meren, omdat op zee de energie-toevoer aan het snelheidsveld een belangrijke konstante komponent van astronomische oorsprong bezit, zodat de energie-inhoud van het snelheidsveld (op verschillende lengteschalen) minder fluktueert dan in meren het geval kan zijn.

Synthetische velden zijn gebruikt van goed gedefinieerde struktuur, zodat numerieke experimenten konden worden uitgevoerd onder beheersbare omstandigheden, wat in de natuur niet mogelijk is. Door de resultaten met experimenten en waarnemingen in het veld te vergelijken, verkrijgt men inzicht in de omstandigheden en mechanismen in de natuur en in de wijze waarop men deze kan modelleren.

De huidige computer-faciliteiten maken het niet alleen mogelijk deze fundamentele onderzoekingen met synthetische velden met een gedetailleerde spektrale struktuur uit te voeren, maar ook om bestaande stromingsmodellen aan te vullen met spektrale komponenten die in het stromingsmodel niet gereproduceerd worden, maar essentieel zijn voor een juiste modellering van verspreidingsverschijnselen. Soms is een meer eenvoudige benadering toelaatbaar, die minder reken-inspanning vergt, maar de spektrale benadering blijft steeds de beste.

Summary

This report presents a study on the behaviour of particle clouds in two-dimensional velocity fields. The results can be applied in a general way but are especially of interest for the dispersion of matter in surface waters of a large horizontal extent and relatively small depth or layer thickness. They may be somewhat more relevant to seas than to lakes, because at sea the energy supply feeding the velocity field contains an important constant component (of astronomical origine) so that the energy content (at various length scales) of the velocity field will not fluctuate as strongly as may be the case in lakes.

Synthetic fields have been used of well defined spectral structure so that numerical experiments could be performed under controlled conditions, which is not possible in nature. By comparing the results with experiments and observations in the field, one obtains insight into natural conditions and prevailing mechanisms and how to model these adequately.

Present computer facilities do not only enable these basic studies with synthetic fields of detailed spectral structure but also make it possible to supplement existing flow models with spectral modes which are not reproduced by the flow model while they are essential for proper modelling of dispersion. Sometimes simpler means to the same end with less computational effort are permissible although they remain inferior to the spectral approach.

Contents

1. Introduction

Velocity fields of large bodies of open water are usually structured in space in a complicated way, showing marked changes on very short and very large distances as well. Some of these features are rather constant, some are changing in time, sometimes in a systematic way, like tidal currents.

For the dispersion of matter, the structure or "organization" in space is quite dominant, as it will be demonstrated in later chapters. One might say that time dependence only affects dispersion phenomena appreciably if it affects the spatial structure strongly and with some persistance. In this context spatial structure can be read as : spectral structure in space, i.e., qualitatively: how strong are the variations in velocities at various distances or "length scales".

In this report, the behaviour of passive particles is considered. In the case of passive transport, the velocity field of the watermass is not affected by the presence of the materials transported. If the unaffected natural field would be known in sufficient detail, no further physical knowledge would be required to predict dispersion patterns. "Any passive particle follows, by definition, the local velocity at its successive positions. It is not necessary to include its Brownian or molecular motion, since the displacements thereby are negligible with respect to the ubiquitous complex 'macroscopic' water motion...". "For all practical purposes it would be no problem if only averages of the velocities over a certain volume (say, 1 liter or even a cubic meter) and certain time intervals (say, of 10 s) would be known. To compute the effect of a continuous release, it would 'only' be needed to make a kinematic computation, releasing a particle, say every second, and computing the path of all particles in small steps of time and space, in accordance to the grid size of the given velocity field. After about 2 weeks (in the 'prototype'), a million positions would have been computed. In spite of the discreteness of the particles and their finite number, for practical purposes the concentration field at that moment would be known in sufficient detail. Carrying on sufficiently long would reveal how long it takes to reach a steady mean in various parts of field and how large fluctuations and periodic changes are around this mean.

One of the purposes of this imaginative exercise is to show that diffusion (molecular or other) has not entered the computation in a quantitative way and qualitatively only at the moments the 'concentration' was reviewed. At those moments it was assumed that limited numbers of particles in relatively small volumes represent a more or less even distribution of a much greater number of molecules of the real pollutant. If more exact estimates are needed, it only means that smaller steps in time and space have to be taken or more particles per second have to be released, which is no objection for an imaginary operation" (VAN DAM, 1982).

The 'thought experiment' of this citation needs not to remain entirely imaginary if we drop the requirement that all velocites should be "real" (measured) or, at least, deterministic (computed in a deterministic model). In any case, velocities should be given on the smallest scale of interest and up. If we can only use grid velocities computed by a two-dimensional flow model, the field contains no structured details below a length scale of several meshes which means that the whole "spectrum" of scales over the entire domain of the model usually ranges less than a factor of hundred and often little more than a factor of ten. An extension with at least the same factor at the side of the smaller scales is most desirable. This can be done in a statistical manner and on a basis of calibration. The statistical representation of the smaller scales is no serious drawback; the precise location of a concentration is usually less important than its value. Further, it may be noted that in the case of a continuous source in a tidal current, pronounced "subgrid" details in the distribution of released matter are caused by the time dependence of the current rather than by its spatial structure (figures 1 and 2).

The important feature of dilution after the moment of release, largely depends upon the spatial structure of the velocity field and can be studied conveniently by considering instantaneous release only. For the purpose of investigating the relations between spectral velocity structure and "dilution" in two dimensions, in chapter 2 synthetic fields will be defined, composed of harmonic functions of space. By modulation of these fields by very slow as well as quite rapid changes in time, it will be shown that the spatial structure of the fields dominates the dispersion process and only most rigidly "frozen" fields may give results that differ significantly from those obtained with similar fields that change in time. Variations in time in our simulation will be only obtained by generation and extinction of spectral components, and not by superimposing periodic or residual velocities. There have been several considerations for this choice. One of them is the aim of maintaining a consistent spectral approach. Addition of 'external' velocities influences the weight of spectral components. Especially velocities of a larger order of magnitude than those of the velocities of the "eddies", reduce the contribution of the concerned eddies to the dispersion by reducing the 'residence time' of particles in the eddies. This has been confirmed by numerical experiments. In addition, the superposition of 'external' velocities and the eddy velocities seems rather unnatural. Especially the smaller eddies will be entrained by a 'main stream' rather than the stream passing through the eddies. By this entrainment, the eddies become material entities: particles largely remain within the eddy during its lifetime. One might argue that by this principle the smaller eddies should be entrained by larger ones and so on. Such a mechanism cannot be realized in an analytic form and had to be abandoned. Afterwards, the results of the simulations do not show a recognizable effect of this (possible) omission. Maybe this is due to the fact that

in each simulation the velocities in all classes of eddies are of the same order and also to the circumstance that possible impacts are repeated on each length scale in a similar way, so that the spectrum is affected uniformly (if att all), with preservation of its structure.

Since the degree of stationarity is adjusted by means of eddy lifetimes and by the fact that the individual spectral components are fixed in space (no entrainment of smaller eddies by larger ones), the case of complete stationarity is contained within the range of tuning.

The above set up has certain consequences when relating the results to experiments in nature, in particular in tidal streams. Dye patches move up and down on the tidal currents over distances which remain larger than the patch diameter for long periods (like 100 to 300 hrs). The history of such a patch is looked at internally, i.e. in a frame attached to the patch itself. Its dispersion is due to the water movements relative to its movement as a whole. This is still true when the patch size becomes larger than the tidal excursion. The velocities corresponding to our numerical model are the "internal" velocities.

Reversely, if the synthetic spectral model has been calibrated on the basis of dye patch experiments and will be used to supplement a given (tidal) flow field (chapter 8), the synthetic "eddies" have to be defined in a frame that moves with the given field.

For marine applications, the restriction to two dimensions is no serious limitation. At the scales on which three-dimensional effects are important or even predominant (scales to one or a few km), they can be modelled by means of a deterministic approach of the vertical structure of horizontal velocities and a relatively simple concept of vertical exchange. When the latter becomes insufficient, this is usually due to stratification problems and a spectral approach would be of little help.

2. Mathematical formulation, numerical procedure.

In the most general case, the two-dimensional velocity fields used in this study are superpositions of a finite number of components of the form

$$u_{x_i} = a_i \cos \left(\frac{2\pi y_i}{\lambda_i} + \phi \right) \qquad (1)$$

in which x_i corresponds to an arbitrary fixed direction in the plane and y_i to the direction perpendicular thereto. λ_i can be called a wavelength and a_i is an amplitude that is constant for a stationary component and time dependent if the component is not stationary. If (and only if) all components are stationary, the entire field is stationary.

The only type of non-stationary components so far used in this study have a finite life cycle with length T (figure 3) during which the amplitude rises smoothly to a maximum and returns to zero according to

$$a(t) = a\left\{1 + \cos\left(\frac{2\pi t}{T} + \Psi\right)\right\} \qquad (2)$$

In all cases where this was applied, a new life cycle of a particular component was started at each moment a(t) became zero, preserving amplitude and wave length, but with a different phase angle ϕ. Further, so far, all components u_{xi} were accompanied by similar components u_{yi}, like formulated earlier (VAN DAM, 1980[a],[b],[c], 1982) as

$$(u_{x_j}, u_{y_j}) = \left[a_j \cos\left(\frac{2\pi y}{\varepsilon_j \lambda_j} + \phi_{x_j}\right), \varepsilon_j a_j \cos\left(\frac{2\pi x}{\lambda_j} + \phi_{y_j}\right)\right] \qquad (3)$$

The simulations reported here have been made with all $\varepsilon_j=1$. One (u_x, u_y)-component of this form (with $\varepsilon_j=1$) constitutes an infinite field of congruent eddies contained in squares on an angle of 45° with the (x,y)-axes (figure 4). A congruent field but with the sides of the squares in the direction of the (x,y)-axes, has a somewhat more complicated analytic form in terms of x and y (PASMANTER 1985, VAN DAM 1985[b]):

$$u_x = a \sin\left(\frac{2\pi x}{\lambda} + \psi_x\right) \cos\left(\frac{2\pi y}{\varepsilon\lambda} + \psi_y\right)$$

$$u_y = -\varepsilon\, a \cos\left(\frac{2\pi x}{\lambda} + \psi_x\right) \sin\left(\frac{2\pi y}{\varepsilon\lambda} + \psi_y\right) \qquad (4)$$

but for our purpose there is no reason to use this formulation.

Initially, all components were defined on the same pair of axes (x,y). This generates a certain degree of order in the velocity field, also if all phase angles ϕ are chosen randomly (figure 5). This order is also reflected in particle tracks (figure 6) if we "freeze" the field (stationary case), but it shows not so clearly in patterns formed by advected blobs of fluid, at least as long as these are still smaller than the largest eddies (figure 7).

Recently, a version of the computer programme was built with arbitrary directions of (x,y) for each eddy component (figure 8). This implies that the paired structure as in (3) and (4) was maintained for the individual components so that the fields can still be completely decomposed into eddies enclosed by squares (ε=1) or rectangles ($\varepsilon \neq 1$). As said before, the option $\varepsilon \neq 1$ was not used so far.

In the most general case, there is no specific arrangement by "eddies" but just a combination of spectral modes of the form (1), with random directions x_i. One may observe that if the number of modes is even, also in this general case the field can be completely decomposed in "eddies" but now of the general form (3) or (4). It is interesting to note, that this can be done in many different ways (if the number of modes is not very small) and that the decomposition can be realized arbitrarily either by quite elongated "eddies" as well as by mixed, or (if the spectrum is dense enough) almost "square" eddies. If the number of modes is odd, the decomposition can be made similarly in many different ways, but now in each case there is one single mode left over.

Of course it is an important feature of the fields mentioned that they all satisfy the continuity condition for a two-dimensional non-compressible fluid,

$$\frac{\partial u_x}{\partial x} + \frac{\partial u_y}{\partial y} = 0 \qquad (5)$$

since each of the constituent modes (1) do so.

If the synthetic fields are to be used to supplement flow fields in flow models of actual situations (varying depth), continuity is not longer strictly given by (5). As long as the variations in depth or layer thickness are relatively small compared with average values, (5) may still be good enough for the supplementary eddy field. In certain cases it may be desirable to replace (5) by the corresponding form with transports $\vec{u}\,h$ (with h = local and temporal water depth) instead of velocities $\vec{u}$ (VAN DAM, 1985[a]).

Numerical procedure

For investigating the transport properties of the velocity fields as defined above, groups of particles were released instantaneously and then advected by the prescribed field. Since there are no other displacements than the advection by the velocity field, there will be no dispersion at all if all particles are instantaneously released at one identical position. The same would be true in physical reality: particles with exactly identical positions are identical particles. Consequently, the particle set has to be attributed a finite initial size. This is done by a preceding ordinary isotropic twodimensional random walk of all particles starting from a single common position, which leads to an isotropic distribution of particles, approaching a normal (gaussian) density distribution with increasing number of time steps and number of particles. For our purposes, the precise shape of the initial distribution thus obtained, is of little importance.

From this initial distribution of finite diameter, the particles are advected by the synthetic non-divergent two-dimensional velocity field only. This is done by displacing the particles one by one in finite time steps, using a simple numerical scheme of first or second order. Using the second order (Runge Kutta) scheme, larger time steps can be taken for obtaining a same accuracy. The accuracy has to be such that a particle follows the movements of the smallest eddies to a sufficient extent. If only the dispersive properties of the velocity field have to be investigated and the field is not rigidly stationary ("frozen"), it is sufficient if the particle remains in the domain of a single eddy (also the smallest) during several time steps, say 10.

If a_1 is the velocity amplitude of the smallest eddy, wave length $\lambda_1 = \lambda_{min}$, the suggested criterion roughly implies

$$\begin{aligned} a_1\, dt &\leqq 10^{-1}\, \lambda_{min} \\ dt &\leqq 10^{-1}\, \lambda_{min}\, a_1^{-1} \end{aligned} \qquad (6)$$

(in fact dependent upon the numerical scheme).

A much stricter criterion has to be applied if the purpose of a calculation is, to show that in a stationary field of the concerned type, most particle trajectories, now coinciding with streamlines, are closed curves (figures 6 and 8) of the size of the largest eddies or smaller. Then the time step length required depends upon the size of the smallest eddy as well as of the largest one, and of course upon velocity as well. The required steps are roughly one to two orders of magnitude smaller than would follow from (6).

The length

$$L = \sqrt{\sigma_x^2 + \sigma_y^2} \tag{7}$$

with

$$\sigma_x^2 = \frac{\sum_{n=1}^{N} (x_n - \bar{x})^2}{N} \qquad \sigma_y^2 = \frac{\sum_{n=1}^{N} (y_n - \bar{y})^2}{N} \tag{8}$$

(N= number of particles)

has been used as the size measure of particle patches.

3. Energy and velocity spectra.

A component of the form (1) has a particular direction x_i. It is assumed however that all directions have equal chances, in other words that the superimposed fields are (averagely) isotropic. This means that the usual one-dimensional formulations of spectra can be applied (MONIN and OZMIDOV, 1985). One may state that any series of wavelengths λ_i or wavenumbers $k_i = 2\pi/\lambda_i$ constitutes a spectrum, but in order to get insight in spectral structures and to be able to compare these with theoretical concepts (usually formulated in a continuous form) a regular spacing of spectral "lines" is required. From a viewpoint of similarity between different scale ranges it seems a logical choice to space the successive wavelengths of the various components by equal factors rather than equal differences. If this is done, it appears that the velocities of the various components are simply related to the usual concept of characteristic velocities or eddy velocities at the various length scales.

The spectral structure of a velocity field in the space domain is often characterized by an energy density function E(k) (kinetic energy per unit mass and unit wave number), which means that if only velocities in a small range of wave numbers, dk, are considered, the (average) kinetic energy of a unit of mass in the field would be

$$dE_{kin} = E(k)\,dk \tag{9}$$

Theoretical forms of E(k) are practically always of the simple type

$$E(k) = c_k\, k^{-m} \tag{10}$$

in which c_k stands for various expressions, depending upon the theory concerned. The best kwown case is probably the kinetic energy spectrum in the

so-called inertial (sub)range of (three-dimensional) turbulence at high Reynolds numbers (m= 5/3),

$$E(k) = C_1 \varepsilon^{2/3} k^{-5/3} \tag{11}$$

in which ε is the rate of energy dissipation, equaling the spectral energy flux (flowing from larger to smaller eddies) and the external supply of kinetic energy (to the largest eddies of the range). There are no good theoretical reasons or empirical evidence that (11) should also hold for the spectrum of horizontal eddies in seas.

To link the kinetic energy concept to dispersion one wishes to derive a typical velocity for a certain length scale (wave length) or corresponding wave number. From a viewpoint of similarity and considering that the required velocity should have relevance to the exchange of water masses at the concerned length scale, it seems appropriate to relate the size of the interval dk in expression (9) to k by $dk = \alpha k$, where α represents a certain fraction ($\alpha \ll 1$). Then

$$dE_{kin} = \alpha k E(k) \tag{12}$$

being the kinetic energy (per unit mass) in the chosen interval, the characteristic velocity at this "scale" should be

$$v_c \sim \overline{|\vec{v}|} \sim \{\alpha k E(k)\}^{\frac{1}{2}} \tag{13}$$

e.g. if E(k) has the form (10), then

$$v_c \sim (\alpha c_k k^{1-m})^{\frac{1}{2}} \tag{14}$$

This defines a spectrum of velocities of the shape

$$\sim k^{\frac{1-m}{2}} \quad \text{or} \quad \sim \lambda^{\frac{m-1}{2}} \tag{15 a,b}$$

in conformity with conventions. For example the well-known case m=5/3 (formula (11)) gives with (15b) the well-known result

$$v_c \sim \lambda^{1/3} \tag{16}$$

Equations (13) and (14) remind to the fact that the velocities v_c contain an arbitrary factor $\alpha^{1/2}$. A particular choice of α with a particular energy spectrum E(k) gives a velocity spectrum in absolute terms and in this way discrete synthetic spectra can be related to given forms of E(k). By spacing the "lines" of discrete spectra by equal factors, their absolute values will depend upon the relative size α^* of the spacing intervals in the same way as v_c depends on α according to (17).

It is generally assumed (MONIN and OZMIDOV 1985 and references therein) that the effective dispersion coefficient of a (two-dimensional) patch of size L (as defined by (9)), defined as

$$K(L) = \frac{1}{4}\frac{dL^2}{dt} \tag{17}$$

is proportional to the size L as well as to the characteristic velocity associated with the length scale $\lambda = L$ in the velocity spectrum:

$$K(L) \sim L \times v_c(L) \tag{18}$$

As we have seen, v_c is defined except for a constant factor. One could use (18) to define v_c in an absolute sense. This becomes more feasible with the availability of a simulation model that provides K(L) for given spectra.

For the spectra of type (10), (18) implies

$$K(L) \sim L^{\frac{m+1}{2}} \tag{19}$$

with the two best known examples

$$m = 5/3 \quad K \sim L^{4/3} \tag{20}$$

$$m = 1 \quad K \sim L \tag{21}$$

corresponding (by (17)) to a growth of L after an instantaneous point release at time t_o as

$$L \sim (t - t_o)^{3/2} \tag{22}$$

and

$$L \sim (t - t_o) \tag{23}$$

respectively.

The numerical simulations with the discrete spectra as described in the foregoing are in agreement with (22) and (23) (figure 9) which can be seen as a confirmation of the conventional assumption (18) as well as of the proper functioning of the simulation model.

The general form of (22), (23) in terms of (10) is

$$L \sim (t-t_o)^{\frac{2}{3-m}} \tag{24}$$

but it should be borne in mind that the above considerations and resulting relationships are only valid within the ranges covered by the spectra of the concerned type (10), i.e. for patches of a size well within the range of length scales covered by these spectra. Other cases will be dealt with in later chapters.

In the numerical experiments described in this report, only spectra of the type (10) have been used and except in the case of figure 9 (m = 5/3 and m = 1) the experiments have been restricted to the case m = 1. In a sense, this can be seen as an arbitrary choice, but there is also the practical consideration that for a long range of scales, spectra with $m \approx 1$ give a quite fair description of dispersion in the North Sea. The range of applicability of a constant $m \approx 1$ has recently even been extended considerably by combining the k^{-1} spectrum for the horizontal eddies with an explicit modelling of the processes in the vertical (vertical velocity profiles combined with vertical exchange).

The case m = 1 is also attractive because of its simplicity. All (average) velocity amplitudes in one spectrum with fractional spacing α^* become mutually equal and the various expressions become even simpler than they already are (for arbitrary m):

$$E_k = c_k\, k^{-1} \tag{25}$$

$$dE_{kin} = \alpha c_k \tag{26}$$

$$v_c \sim (\alpha c_k)^{1/2} \tag{27}$$

and as far as L is within the spectral range:

$$L \sim (t - t_o) \tag{28}$$

for patches resulting from instantaneous point release.

It was said earlier that only instantaneous 'point' sources have been studied, although a finite initial patch size is necessary. In practice the initial size has a lower bound set by the finite length of the spectral range. If it would be taken (much) smaller than the smallest eddy the patch would initially not only be dispersed very slowly but also be stretched into thready shapes which would be an unadequate initial condition for the later process within the spectral range. The finite initial size implies that the theoretical point of time t_o of (24) and (28) in fact lies before the start of the simulation. The patch always starts with a specific "age" with respect to t_o. Only if in the double-logarithmic plot of L as a function of t the initial age is correctly estimated, L (t) will show as a straight line (apart from deviations due to the stochastic aspects of the simulations). It can be noted that in most cases (figures 9, 12, etc.) the initial position of L(t) is indeed not precisely chosen on the straight line that should be expected with a proper time scale. Because of the logarithmic scale, the small shift in time soon becomes unnoticeable when time proceeds. The effect is similar to what happens when the release time (of a finite patch!) of a dye experiment is identified with the start of a theoretical instantaneons point release. If in a graph, the measured curve deviates from the theoretical one with a constant time shift (for larger times rather soon becoming invisible in the logarithmic plot), it means in fact that the two functions are identical.

4. Variability in time.

Perfectly stationary velocity fields do not occur under natural conditions and certainly not in surface waters. This could be a good reason to leave them out of consideration. Indeed, although touched briefly in this chapter, they will remain a theoretical extreme of the cases to be viewed.

In (realistic) non-stationary fields, usually a certain degree of stationariness can be discerned. Especially for the larger eddies some persistency is quite likely and will also exert more influence on observed transport phenomena than small eddies could do. In general, large eddies live longer than small ones and in most simulations the lifetimes were taken proportional to the size of the eddies. In the usual case m = 1, this means that the lifetimes are equal in terms of the number of revolutions. In this chapter the possible influence of the degree of variability/stationariness on dispersion will be investigated.

The (unrealistic) case of complete stationarity (infinite lifetime of all eddies) is of some interest for understanding the influence of lifetimes upon dispersion. When individual particles are released on arbitrary locations of a stationary field consisting of say 5 to 8 eddy components of type (3) it appears that a majority of these particles follow closed trajectories (figures 6 and 8) and to such an extent that most of the surface area in the plane is enclosed by such contours. Because of the stationariness the

trajectories coincide with streamlines. An area enclosed by a closed streamline, can only contain streamlines that are closed as well. Initially it was believed that in fact all streamlines in fields composed of stationary components of type (3) were closed and that exceptional trajectories crossing the area analyzed, might be numerical artefacts caused by singularities which in fact only were boundaries of zero thickness, separating zones with "normal" eddy structures. In a later experiment (figure 8) it appeared that the longer trajectories were not so exceptional and that under considerable reduction of time step size, most of them remained completely stable and apparently were quite real. Then the area of computation was widened and it was found that several of the seemingly open tracks closed within a larger domain than first considered. It is now clear that although most streamlines are closed around an area of the size of the largest eddies or smaller, a number of tracks covers a much greater surface, enclosing several areas of the size of the largest eddies. It remains possible that in fact all streamlines are closed but this can never be proven by calculating (finite numbers of) particle tracks. A theoretical proof has not been found either, even for the case of equal orientation of all (x_i, y_i).

A general proof of the kind here suggested, is not essential for our practical purposes. The factual data obtained with the stationary field are sufficient evidence for understanding the results obtained with gradually increasing lifetimes of eddies (figures 10 and 11). If for infinite lifetimes all tracks would close within areas of the order of the largest eddies or smaller, dispersion in the stationary field would be blocked at length scales L of the same order as λ_{max} or smaller. After it was found that certain tracks extend over much larger areas, it can be understood that the blocking occurs indeed in certain cases, but not always (figures 10 and 11). The figures show that, at the other hand, a certain degree of trapping may also occur when lifetimes are not quite infinite but long compared with the period observed. This is of course what should be expected. It is of more importance that the initial cloud lies entirely within a closed streamline than that this streamline is strictly stationary. If its lifetime is longer than the observed period, an effect of trapping should be obvious. The fact that in perfectly stationary fields the cloud may extend over much larger distances than λ_{max} is a warning against fast conclusions on the basis of L(t) - plots only. A few particles travelling far beyond the range within which most other particles remain captured, may cause L-values of the same order as when all particles were spread over the larger distance. An (almost) "normal" rate of spreading only measured by L(t) is therefore no good evidence for actual normal dispersion. To find out whether longer lifetimes do not yet impede dispersion compared to shorter lifetimes, we will have to look at the character of the distribution as a whole rather than at a rough measure like L(t). For many other purposes the quantity L is good enough.

5. Spectral density, spectral gaps and cut-off.

The synthetic, superpositional character of the artificial fields implies that they are composed of a finite number of modes (formula (1)) or eddy classes (formula (3)) so that we might speak of a "line spectrum". In this chapter the question is considered to how the dispersion properties of the fields depend upon the density of the spectral lines. This is closely related to the effects of spectral gaps and cut-off.

In figure 12 it is shown that cutting off a spectrum of some given density at a certain maximum wave length, rather results soon into a classical diffusion behaviour of the dispersion process: patch diameter increasing with the square root of time (EINSTEIN 1905, CRANK 1967, and many others). The level of the $t^{1/2}$ - line, corresponding with the value of the diffusivity K, rises with increasing density (preserving the velocity amplitudes of the individual components) of the cut-off spectrum. If we replace the cut-off by a "cut-out" or gap of sufficiently large width, the same effect will occur at the lower end of the gap. The larger eddies at the other end will initially have no influence if they are sufficiently "far away": then the velocity field they form is virtually uniform within the small area covered by the particle cloud near the low end of the gap. When the cloud grows larger, the large eddies will gradually cause a steeper increase of cloud size L(t) (figure 13). The figure shows that the gap has to be rather wide to have a clear influence shown by a noticeable dip in the L(t) curve.

It is interesting to see how the constant value of K, reached so soon after L has become $> \lambda_{max}$ (figure 12), depends upon the features of the underlying spectrum.

It should be expected that if there is only one eddy field of type (3) with amplitude a and wavelength λ, and yet stationarity is avoided in some way (to prevent trapping of particles), the resulting value of K will be

$$K = k_o \, a \, \lambda \tag{29}$$

in which k_o is a dimensionless coefficient. If there are several eddy components with mutually quite different wavelengths $\lambda_1, \lambda_2, \ldots \lambda_J$, the dispersive effect of each of them will be almost independent of that of the others. In that case the total diffusivity would be given by

$$K = k_o \sum_{j=1}^{J} a_j \, \lambda_j \tag{30}$$

In the case m = 1:

$$K = k_o \, a \sum_{j=1}^{J} \lambda_j = \frac{1 - (f_\lambda^{-1})^J}{1 - f_\lambda^{-1}} \; k_o \, a \, \lambda_{max} \tag{31}$$

(f_λ = ratio between successive values of λ_j)

On the other hand, if all λ_j would be the same, there would be a partial mutual extinction of the different components and we should expect

$$K = k_o^* a \sqrt{\lambda_1^2 + \ldots + \lambda_j^2} = k_o^* a \lambda \sqrt{J} \qquad (32)$$

rather than $k_o a \lambda J$ as would follow from (31).

Also in a spectral range with rather small distances between the wavelengths λ_j, it should be expected that there is some interference and the ratio between K and $\sum a_j \lambda_j$ (or $a \sum \lambda_j$) will become smaller than k_o in (30) and (31).

The ratio between K and $\sum a_j \lambda_j$ has been determined for all simulations of this type performed so far (table 1). In all cases $\sum a_j \lambda_j = a \sum \lambda_j$ (spectrum of type (10) with m=1). The number of wavelengths per (logarithmic) decade ,N, ranged from 4 to 16, so the constant factor f_λ between successive values ranged from $10^{1/4}$ to $10^{1/16}$ and the relative "channel width" $\alpha^* = f_\lambda - 1$ from 0.7783 to 0.1545. It is remarkable that the expected decrease of the ratio k with increasing density N does not show, even at the level of N=16 ($f_\lambda = 10^{1/16} = 1.1545$) although the spread in the figures is quite small (table 1).
Apparently, the decrease at this level is still smaller than the spread of about 7 % (first 3 groups of 3 computations only). So we may conclude that the average 0.0357 of the first three groups of computations is a good

Table 1

Number of computations	Number of wavelengths per decade N (*)	Factor f_λ between successive wavelengths f_λ	relative channel width α^* ($=f_\lambda - 1$)	Total number of components	Ratio $k = K : (a\sum\lambda)$
3	4	$10^{1/4}$	0.7783	8	0.0345
3	8	$10^{1/8}$	0.3335	8	0.0390
3				15	0.0326
4	16	$10^{1/16}$	0.1545	29	0.0387

(3 and 3 → 0.358)

(*) In these simulations, number of selected wavelengths per decade and number of "components" (of form (3)) per decade are identical

estimate of the dimensionless factor k_o of the expressions (30) and (31).

With the value of k_o, thus derived, dispersion coefficients K in the range $L > \lambda_{max}$ can be determined for various situations. An interesting case is the asymptotic value of K for $J=\infty$ with a given velocity amplitude a (or spectrum a_J) and a given $\lambda_{max} < L$.

For a given relative spectral line distance α^* and a given λ_{max}, the expression (30) voor K will usually have a finite value for $J\to\infty$. This is certainly so for the case (31) where the summation amounts to a geometric series. Its limit for $J \to \infty$

$$K_\infty = k_o\, a \lim_{J\to\infty} \sum_{j=1}^{J} f_\lambda^{1-j} \lambda_{max} =$$

$$= k_o a\, \lambda_{max}\, f_\lambda\, (f_\lambda - 1)^{-1} = k_o\, a\, \lambda_{max}\, (\alpha^*+1)\, \alpha^{*-1} \qquad (33)$$

Some examples with the above value $k_o = 0.0357$, with the choice $\lambda_{max} = 1000$, a=0.05 and with the same spectral densities as in table 1, are given in table 2. The added case J=1 should be seen as a theoretical limit at the lower end of the range of the number of components, J, since for one component, non-stationarity cannot be obtained in the same way as for $J>1$.

N	one component (J=1)(formula (30))	N components (upper decade) J=N (see (34))	J= ∞ (formula (33))
4	K=1.785	3.671	4.0785
8	1.785	6.423	7.1396
16	1.785	11.98	13.317

$[L^2]\,[T^{-1}]$
(any units)

Table 2

The contribution of the upper decade (0.1 λ_{max} to λ_{max}) amounts to exactly 90% of the total of K, since for J terms (the sum of) a geometric series equals the limit for $J=\infty$ multiplied by $1-r^J$. In this case

$$1 - r^{J=N} = 1 - (f_\lambda^{-1})^N = 1 - \{(10^{1/N})^{-1}\}^N = 1 - 10^{-1} \qquad (34)$$

So if the spectrum does not extend indefinitely at the side of the smaller wavelengths, the contribution of the part below the upper decade is even smaller than 10%.

It should be expected that with further increase of the density of the spectral components, the linear relationships (30), (31) will not remain valid. If the number of components within a certain range is increased further, K will gradually increase slower than proportional to the number of components and the dependence upon N will finally tend to a square root relationship like (32). Apparently, the densities used so far, are too small to demonstrate this.

In the range $\lambda_{min} < L < \lambda_{max}$, the situation is quite different. At the same relatively low densities of spectral modes as above, no apparently linear relationship between K and the individual contributions of single modes was found, in complete agreement with theoretical considerations.

In the range $\lambda_{min} < L < \lambda_{max}$, K is not a constant for the whole spectral range, but it is proportional to $L^{\frac{m+1}{2}}$ (formula (19)), so for m=1, it is proportional to L:

$$K(t) \sim L(t) \tag{35}$$

and since form m=1, $L(t) \sim (t-t_o)$ (formula (28)), also

$$K(t) \sim (t-t_o) \tag{36}$$

So the investigation of the influence of spectra on K and or L in the case m=1 is completely equivalent and amounts to investigating the behaviour of P in

$$L(t) = P \times (t-t_o) \tag{37}$$

where P is a velocity. The notation P has been chosen after JOSEPH and SENDNER (1958) who have used it in essentially the same sense.

Figure 14 represents the results of a number of numerical experiments with m=1 in the range $\lambda_{min} < L < \lambda_{max}$ for various densities of spectral modes but a fixed value (=0.05) of the velocity amplitude a in all cases. This a, in terms of (27) is equivalent to a fixed velocity v_c^* in a channel of variable width α^* and by (27)

$$c_k \sim v_c^{*2} / \alpha^* \tag{38}$$

in agreement with the fact that the energy density will increase if more components of the same intensity are taken within a fixed range. The energy within one channel α^*

$$dE^*_{kin} = \alpha^* \, c_k \sim \alpha^* \, \frac{v_c^{*2}}{\alpha^*} = v_c^{*2} \tag{39}$$

is in all cases the same, but in a fixed channel width α

$$dE_{kin} = \alpha c_k \sim \frac{\alpha v_c^{*2}}{\alpha^*} \sim \alpha^{*-1} \tag{40}$$

The velocity v_c associated with such a fixed channel is a measure for K(L) for given L (formula (18)) and (since m=1) also for P (=2K:L for all t). By (40)

$$v_c \sim \alpha^{*-\frac{1}{2}} \tag{41}$$

So that we may expect

$$P \sim \alpha^{*-\frac{1}{2}} \tag{42}$$

P has to be found from the data represented in figure 14. The figure illustrates that for relatively small t, a systematic influence of the density (c.q. channel width) is obscured by the stochastic elements in the simulation. At large t, the stochastic effects gradually average out and at the end ($t-t_o=10^7$), all curves are arranged in the expected order and the best way to estimate P seems to consider just these final values of L which ideally should equal $P\times10^7$. In figure 15 the thus obtained values P (α^*) are plotted against $\alpha^{*-1/2}$and the result seems a fair confirmation of the theoretical expectation (42). Later, the data set was somewhat extended; the results plotted in the same way, are shown in figure 16.

The relation between v_c and α^* is not linear and the relation between v_c and the number of modes per decade or other fixed (logarithmic) interval is not either. The relation between α^* and such a density d_r (r refers to the ratio between the boundaries of the interval) is

$$(\alpha^*+1)^{d_r} = r \ (=\text{constant}) \tag{43a}$$

$$\text{or } \log(\alpha^*+1) \sim d_r^{-1} \tag{43b}$$

For high densities d_r (small α^*) this relation tends to an inverse proportionality and then (42) could be replaced by $P \sim \sqrt{d_r}$; in the available material the densties are just too low to justify this approximation. The plot of P against $\sqrt{d_r}$ (fig. 17) differs indeed from figures 15 and 16, although it just happens not to be so evident that the correlation is indeed worse, as should be expected.

For m=1, the definition of K (equation (17)) implies $K \sim L\times P$ while at the same time $K \sim L\times v_c(L)$ by (18). It is clear that in this case v_c does not depend upon L, but it does contain an arbitrary factor (αin equation (27)). So P is a possible choice for a specific value of v_c, determining a value α_p

of α by (27):

$$P^2 = \alpha_p c_k \quad \text{or} \quad c_k = \alpha_p^{-1} P^2 \tag{44}$$

From $dE_{kin}^* = \alpha^* c_k$, the kinetic energy in one channel α^* (containing one spectral component), c_k can be computed. The spectral component in the present simulations is of type (3) with all $\varepsilon_j = 1$ and all $a_j = a(t)$ as prescribed by (2). Taking the probably most reliable value of P (case N=16 in the set of figure 14) and after computing c_k for this case (using (1) with (2), squaring, averaging etc.) we find $\alpha_p = 0.157$ or

$$c_k = 6.4\ P^2 \tag{45}$$

There is no point in writing this estimate with a larger number of digits.

6. Patch shapes.

6.1 "External" shape.

Our particle clouds are statistical representations of "patches" containing a much larger number of dispersing elements, such as dissolved molecules in a patch of pollutant or in a cloud of tracer. For example, in a common rhodamine tracer experiment at sea there will be a number of rhodamine molecules of the order of 10^{25} or 10^{26}. Of course, to define the essential 2D horizontal characteristics of the distributions a representative sample containing a much smaller number of particles will be sufficient.

If only a general length measure such as L (equation (7)) is to be investigated, the number of particles can be very small. In the studies of L(t) reported in the preceding chapters, the number of particles in most cases was only 50. No extra information on L (t) would be gained when a larger number would be used. The rather great deviations of L(t) relative to the average behaviour and correspondingly among individual simulations can be attributed to the limited number of spectral modes and their intermittency in time with mutually random phase (e.g. figure 18 A and B with 2 and 4 components per decade respectively and figure 14 with 2,4,8 and 16 components). Indeed a tendency to smoother curves and smaller mutual differences for higher density of spectral components can be noticed, but the available number of computations is still rather limited. There is a clear tendency of convergence and smaller deviations for larger times. One of the reasons is the very small number of "active" modes in the initial stages. In fact, it might have been better to start with somewhat larger patches with the same values of λ_{min}. A further extension of the spectra to smaller wavelengths would have the same effect without reduction of the range of computation, but meets serious problems of computation times.

Also patch shapes are in the initial stages less regular than later, (figure 19) due to the initially small number of active modes. This situation is somewhat artificial but at the other hand, also in nature rather odd shapes may be found. Apparently the real spectra are not always smooth and simple.

Beside the studies of particle clouds, in a number of simulations the development of closed (initially circular) contours was followed (figures 7 and 20). In fact there is a close relationship between evolving contours and clouds of particles (figure 20). In the figure the initial circle is somewhat smaller than the cloud of particles released at the same time in the same velocity field, but the particle cloud becomes gradually arranged in a similar fashion. If a second circle, just enclosing the entire cloud would have been released, this contour would have developed in a similar way as the smaller one, but would always keep the particles of the cloud enclosed.

The contours become soon untractable by computer simulation but the unlimitedly growing particle patches considered in preceding chapters remain enclosed by such contours at any time and the surface area within these contours is rigidly constant. The unlimited growth in extension of the patch and the increasingly regular distribution of the enclosed particles, implies a tremendous growth of contour length and an inconceivable fine threadiness at large times. It is clear that at some moment even a minute molecular diffusion is sufficient to "erase" the very thin threads and homogenize local distributions. But also without such a mechanism the inhomogeneities will at some time become imperceptible on a macroscopic level, which illustrates the minor importance of molecular diffusion in this kind of processes.

The development of this type of contours has relations with chaos theory. The contour length grows exponentionally in time (LICHTENBERG & LIEBERMAN, 1983; BROWN, 1988) except for long times in stationary fields.

6.2 "Internal" Shape.

After it was seen that on microscopic scales "contouring" may lead to extremely involved patterns, it can be observed that after some time the particle distributions become smooth enough to allow the construction of zones separated by "contours" of particular concentrations, provided that many more particles are released than needed to study $L(t)=\sqrt{\sigma_x^2(t) + \sigma_y^2(t)}$. The question of the "internal" distribution of concentrations in clouds generated in turbulent and other eddy fields has already attracted much theoretical interest in the past(JOSEPH & SENDNER, 1958; OKUBO, 1962[a],[b]; OZMIDOV, 1958, 1968; PASMANTER, 1980; SCHÖNFELD, 1962; TALBOT & SENDNER, 1973; VAN DAM, 1980[a], 1982). Quite a few different distributions have been proposed (JOSEPH & SENDNER, 1958; NEUMANN & PIERSON, 1966; NIHOUL, 1975; OKUBO, 1962[a],[b]; OKUBO & PRITCHARD, 1960; SCHÖNFELD, 1962) but the value and theoretical significance of these functions is not very clear.

A first result from numerical simulation in an artificial eddy field has been published by VAN DAM (1982) but the way of obtaining the distribution function can be criticized (figure 21). The distribution shown is more pointed than the gaussian and this feature it has in common with most theoretical predictions. At sea, measured distributions seem to be rather variable, even during one experiment (VAN DAM & SYDOW 1970, WEIDEMANN (ed.) 1973) but the rather complex patch shapes (maybe poorly reconstructed from the limited number of cross sections) justify some doubt in most cases, so that a numerical simulation still seems an attractive alternative. It was tried recently to improve the result of 1982 (1000 particles) in a simulation of 2000 particles, but this still gives results that are too sensitive to the way of analyzing particle positions, although again there seems to be some preference for distributions more pointed than the gaussian (figure 22).

At present, for a better result a very large computation with more particles and longer simulations time seems necessary but there are some doubts about the priority of such an exercise and the possibilities of a meaningful interpretation.

7. Application to North Sea data.

Several authors have already concluded that patch diffusion in the North Sea can reasonably well be described with (24) with a value of the exponent of $(t-t_o)$ close to 1, which means in terms of an energy spectrum of type (10) a value of m close to 1. Usually the exponent $\frac{2}{3-m}$ of $(t-t_o)$ was estimated a little larger than 1, which would imply that also m would be somewhat larger.

Recently, simulations have been performed with explicit modelling of the processes in the vertical, which dominate the dispersion of patches up to sizes of one to a few km. In the same simulations, the dispersion by horizontal eddies was modelled with an isotropic process corresponding to m=1. The curves resulting from combining the two mechanisms, compared with data sets like figure 23 give no good reason for taking m somewhat smaller or larger than 1 as long as one general value of m is used, without differentiation between various parts of the North Sea.

The description with m=1 implies a behaviour of $L \sim (t-t_o)$ for large scales (beyond the range of influence of the vertical processes) and the present estimate of P (defined by (37)) on basis of the data set of figure 23 is $P=0.0067\ ms^{-1}$ and by (45) we find $c_k=2.87\times10^{-4} m^2 s^{-2}$.

Summarizing, a fair simulation of dispersion in the North Sea can be obtained by modelling the processes in the vertical, combined with a simulation that conforms with a simple energy density spectrum of horizontal eddies

$$E_k=2.87\ 10^{-4}\ k^{-1}\ m^3 s^{-2} \qquad (46)$$

corresponding to a value of diffusion velocity P as defined by (37)

$$P=0.0067\ ms^{-1} \tag{47}$$

Typical eddy diffusivities for large t follow from

$$K=\tfrac{1}{2}P^2(t-t_o)=\tfrac{1}{2}PL \tag{48}$$

In initial periods of the order of one day (and often longer) the effective K will be larger than would follow from (48), caused by shear dispersion due to vertical velocity shear and vertical exchange.

The above approach is quite global and does not account for local differences. It is likely that c_k will be smaller in regions of weaker tidal flow, the tides being one of the important sources of energy to the spectrum of velocity variations as a whole. ZIMMERMAN (1978) has described how vorticity at particular scales is generated by the interaction between the tides and the topography structure of the bottom at related length scales.

Experiments indicate that also in time there may be important variations in spectral energy distributions, but it is often difficult to distinguish the part of the dispersion due to vertical shear from that of the purely horizontal structure. Especially if there is some stratification, these effects influence the total dispersion for a long period, up to several days.

In figure 24 an example is given in which it is clear that at least some dispersion agent has disappeared or sharply decreased in time: from t_a to t_b, L increases with and exponent of t, much smaller than 0.5, the minimum that is possible with an averagely stationary spectral structure. One should keep in mind however that is is only evident that the mechanism has disappeared or strongly decreased within the area of the patch. But the patch has been displaced in the meantime and the possibility should be left open that this is the main cause of extinction of the concerned agent within the patch.

8. Concluding remarks.

Dispersion in two dimensions can be simulated just by advection, in a realistic fashion. This technique avoids the problems of gradient type diffusion concepts which are known to be incorrect except in wide spectral gaps that usally do not exist in the range to be modelled. The technique also avoids paradoxes such as arise with random walk techniques, also if the latter are refined by application of "scaling" in tune with the spectral structure of the velocity fields (VAN DAM, 1982, 1985[b,c,d], 1986).

Because of these two fundamental properties, the advective approach is the ideal way of modelling dispersion from the physical point of view. Disadvantages are of purely practical nature and concern the amount of computational effort.

If a reliable numerical flow model is available, the best results will of course be obtained if the complete velocity structure generated by this model is utilized in the computation of the advection of matter and only the modes that are absent or too weak in the computed flow field are supplemented by a synthetic eddy field. Subgrid modelling is easy but only feasible by using discrete particles to represent the dispersing constituents. An example in which the subgrid modelling has indeed been performed by means of additional spectral modes, is presented in figure 25.

In practice, it will often be unavoidable to apply more economical techniques and the results may in many cases be acceptable. The availability of a fundamentally better method however facilitates a critical use of other means and can in many instances provide valuable supplementary information such as on fluctuations and spatial variability of concentrations.

Acknowledgement

Thanks are due to Mr.P.v.d. Stap for many computations on the CRAY-XMP computer and for converting programmes to CRAY.

References

BROWN, M.G., 1988. Passive tracer disposal in a turbulent two-dimensional flow with large Péclet number.
Submitted for publication.

CRANK, J., 1956. The mathematics of diffusion. Clarendon Press, Oxford, 1-347.

EINSTEIN, A. 1905. Über die von der molekularkinetischen Theorie der Wärme geforderte Beweging von in ruhenden Flüssigkeiten suspendierten Teilcnen. Ann. Phys. (Leipzig), 4 (17): 549-560.

JOSEPH, J. & H. SENDNER, 1958. Über die horizontale Diffusion in Meere, Deutsche Hydrogr. Z., 11: 49-77.

LICHTENBERG, A.J. & M.A. LIEBERMAN, 1983. Regular and stochastic motion. Springer, New York, 1-499.

MAIER-REIMER, E., 1973. Hydrodynamisch-numerische Untersuchungen zu horizontalen Ausbreitungsvorgängen in der Nordsee. Dissertation Univ. Hamburg/Mitteilungen Inst. für Meereskunde der Univ. Hamburg, XXXI: 1-56 + fig.

MONIN, A.S. & R.V. OZMIDOV, 1985. Turbulence in the Ocean. D. Reidel Publ. Co., Dordrecht, Boston, Lancaster: 1-247.

NEUMANN, G. & W.J. PIERSON, 1966. Principles of Physical Oceanography. Prentice-Hall, Englewood Cliffs, N.J., 1-545.

NIHOUL, J.C.J., 1975. Passive dispersion models. In: Modeling of Marine Systems, J.C.J. Nihoul ed., Elsevier Sci. Publ. Co., Amsterdam, 69-95.

OKUBO, A., 1962[a]. A review of theoretical models for turbulent diffusion in the sea. J. Oceanogr. Soc. Japan, 20: 286-320.

OKUBO, A., 1962[b]. Horizontal diffusion from a instantaneous point source due to oceanic turbulence. Chesapeake Bay Inst., Tech. Rep. No. 32, The John Hopkins Univ., 1-123.

OKUBO, A. & D.W. PRITCHARD, 1960. Unpublished note (see D.W. Pritchard, The application of existing oceanographic knowlegde to the problem of radioactive waste disposal into the sea. In: Proc. Symp. Disposal of Radioactive Wastes, IAEA, Vienna, 229).

OZMIDOV, R.V., 1958. On the calculation of horizontal turbulent diffusion of the pollutant patches in the sea.
Dokl. Akad. Nauk, SSSR, 120: 761-763.

OZMIDOV, R.V., 1968. Horizontal turbulence and turbulent exchange in the ocean. Publ. House "Science", Moscow (in Russian): 1-199.

PASMANTER, R.A., 1980. Diffusion in highly turbulent fluids. Phys. Lett. A75: 366-369.

PASMANTER, R.A., 1985. Dynamical Systems, Deterministic Chaos and Dispersion in Shallow Tidal Seas. Rijkswaterstaat, Directie Waterhuishouding en Waterbeweging (The Netherlands), Physics Division. Report ("nota") FA 8505: 1-34.

SCHÖNFELD, J.C., 1962. Integral Diffusivity. J. Geophy. Res. 67: 3187-3199.

SUIJLEN, J.M., 1975. Turbulente diffusie in het IJselmeer bij Medemblik, gemeten met behulp van rhodamine-B. Rijkswaterstaat, Directie Waterhuishouding en Waterbeweging (The Netherlands), Physics Division. Report ("nota") FA 7501: 1-27 (+fig.).

SUIJLEN, J.M., J.S. SYDOW, C. HEINS & P.C. BEUKENKAMP, 1988. Meting van turbulente diffusie en reststromen in de Zuidelijke Noordzee met merkstof-experimenten in 1982. Rijkswaterstaat, Dienst Getijdewateren (The Netherlands). Report in preparation.

TALBOT, J.W. & H. SENDNER, 1973. Consideration of the horizontal diffusion process during the experiment. In: The ICES diffusion experiment RHENO, 1965, (H. Weidemann ed.). Conseil Internat. pour l'Explor. de la Mer, Charlottenlund Slot, Denmark. Rapp. et Proc. Verbaux des Réun., 163, 59-75.

VAN DAM G.C., 1980[a]. Models of dispersion in the sea. Rijkswaterstaat, Directie Waterhuishouding en Waterbeweging (The Netherlands), Physics Division. Report ("nota") FA 8006: 1-130.

VAN DAM, G.C., 1980[b]. Scale dependent dispersion of distinct particles in an artificial eddy field. Fysica van Getijdegebieden, Colloq. NIOZ, Texel (1980). Rijkswaterstaat, Directie Waterbeweging en Waterhuishouding (The Netherlands), Physics Division. Report 07 80-FA: 1-6.

VAN DAM, G.C., 1980[c]. Verspreidingsverschijnselen. Chapter 4 in: Waterbeweging en menging in het zuidelijk gedeelte van de Noordzee. Eindverslag MLTP-4 (G.C. van Dam, editor).
Rijkswaterstaat, Directie Waterhuishouding en Waterbeweging (The Netherlands), Physics Division. Report ("nota") FA 8005: 70-112.

VAN DAM, G.C., 1982. Models of dispersion. Chapter 2 in: Pollutant transfer and transport in the sea (G. Kullenberg, editor). CRC Press Inc. , Boca Raton, Florida, Vol.I: 91-160.

VAN DAM, G.C., 1985[a]. Het probleem van het afleiden van kontinue snelheidsvelden uit op roosters gegeven komponenten. Het stationaire geval. Rijkswaterstaat, Directie Waterhuishouding en Waterbeweging (The Netherlands), Note ("notitie") 85-FA-298: 1-8.

VAN DAM, G.C., 1985[b]. Aspekten van tweedimensionale transportberekeningen voor oppervlaktewateren door middel van passieve deeltjes-simulatie. Rijkswaterstaat, Directie Waterhuishouding en Waterbeweging (The Netherlands), Physics Division. Report ("nota") Fa 8504: 1-33.

VAN DAM, G.C., 1985[c]. A particle model applied to the Western Scheldt. Liverpool conference on mixing and disperion in estuaries (24-25 Sept.). Rijkswaterstaat, Directie Waterhuishouding en Waterbeweging (The Netherlands), Physics Division. Note ("notitie") 85-FA-226:1-4.

VAN DAM, G.C., 1985[d]. Deeltjesmodellen, 2DH. Rijkswaterstaat, Directie Waterhuishouding en Waterbeweging (The Netherlands), Physics Division. Report ("nota") FA 8507:1-44.

VAN DAM G.C., 1985[e]. Contribution to Delft Hydraulics report to the government (classified).

VAN DAM G.C., 1986. Particle modelling of 2DH transport phenomena in the Western Scheldt Estuary. Abstracts Internat. Symp. on Physical Processes in estuaries, The Netherlands: I.1-2.

VAN DAM, G.C. & J.S. SYDOW, 1970. Een diffusie-experiment op 10 km uit de Nederlandse kust ter hoogte van Ter Heijde. Rijkswaterstaat, Directie Waterhuishouding en Waterbeweging, Mathematisch-Fysische Afdeling, nota MFA 7003: 1-28, + fig.

WEIDEMAN, H. (editor), 1973. The ICES diffusion experiment RHENO 1965. Conseil Internat. pour l'Eplor. de la Mer, Charlottenlund Slot Denmark. Rapp. et Proc. Verbaux des Réun., 163: 1-111.

ZIMMERMAN, J.T.F., 1978. Topographic generation of residual circulation by oscillatory (tidal) currents. Geophys. Astrophys. Fluid Dynamics, 11: 35-47.

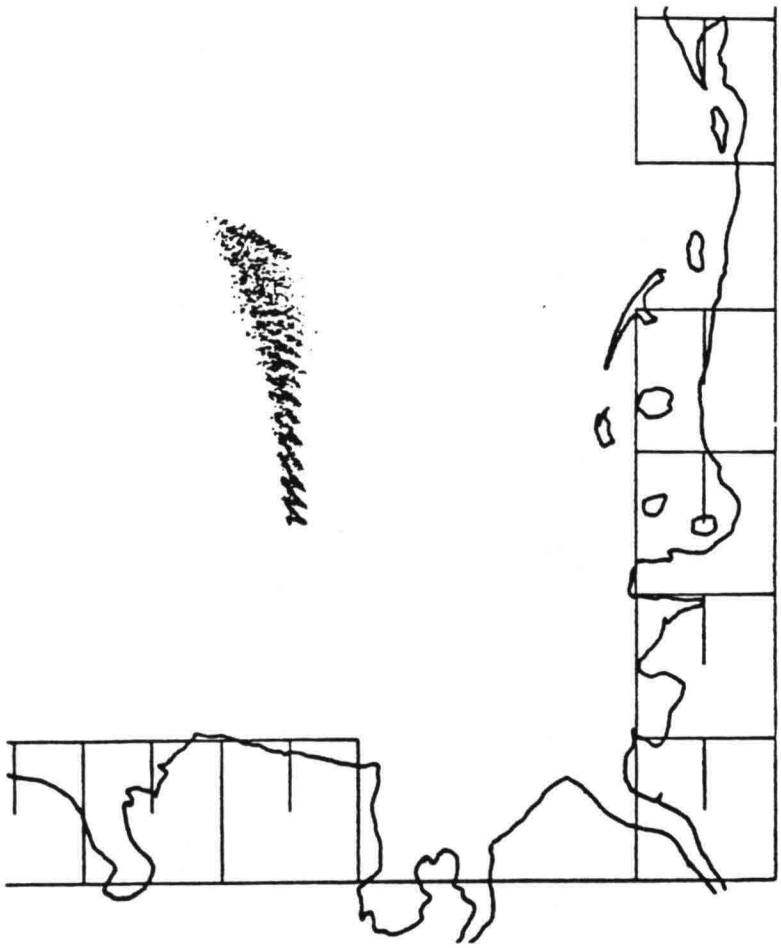

Figure 1 In the case of a continuous source in a tidal current, pronounced sub-grid details are caused by the time dependence of the current.
Example from MAIER-REIMER, 1973

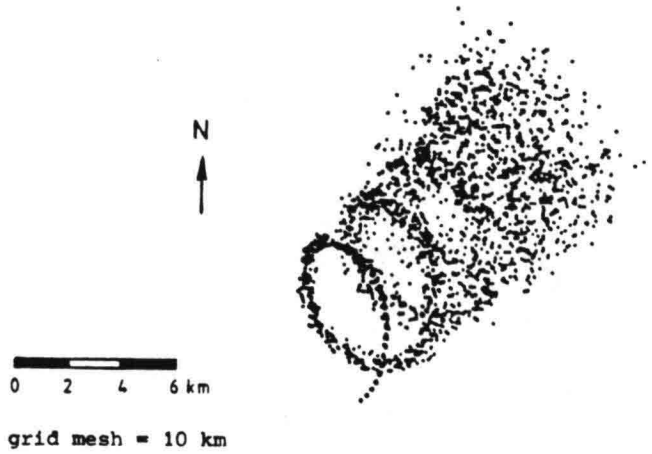

Figure 2 In the case of a continuous source in a tidal current, pronounced sub-grid details are caused by the time dependence of the current.
Example from VAN DAM, 1985[d]

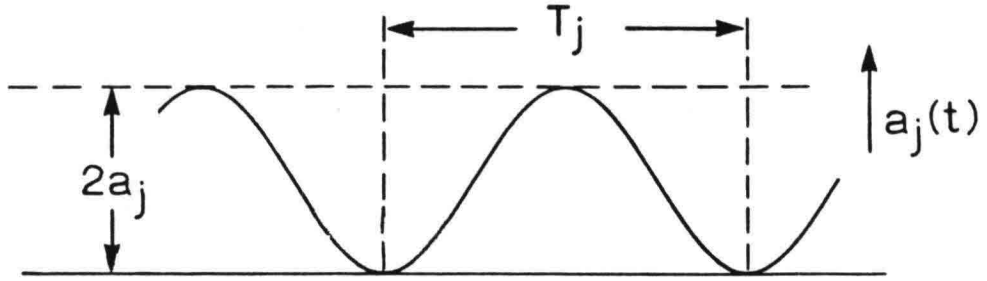

Figure 3 Change of velocity amplitude in time, in non-stationary version of eddy simulation model.
Phases $\phi_{x,y}$ make random jump at times with a(t)=0

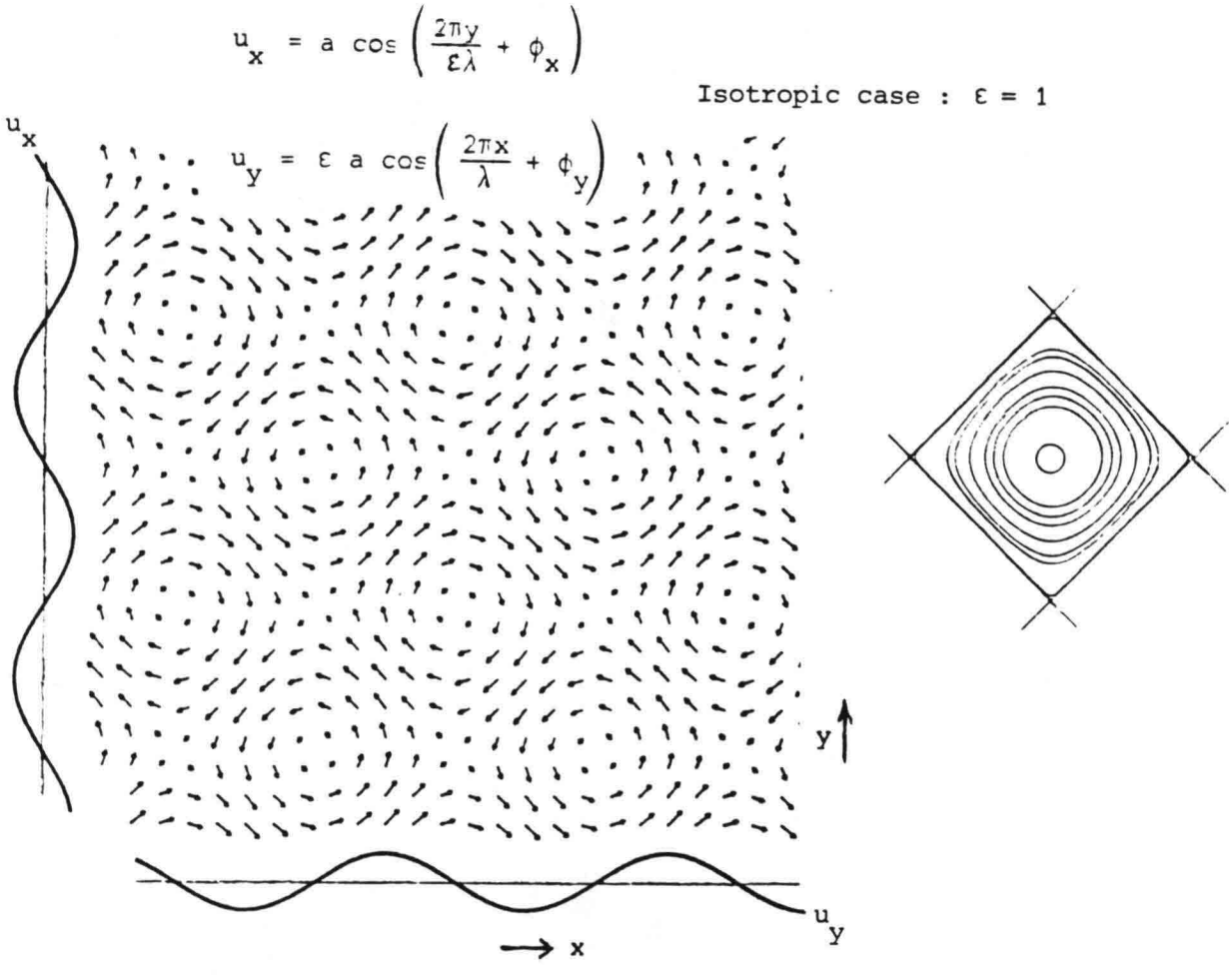

Figure 4

One (u_x, u_y) "component", composed of two orthogonal modes

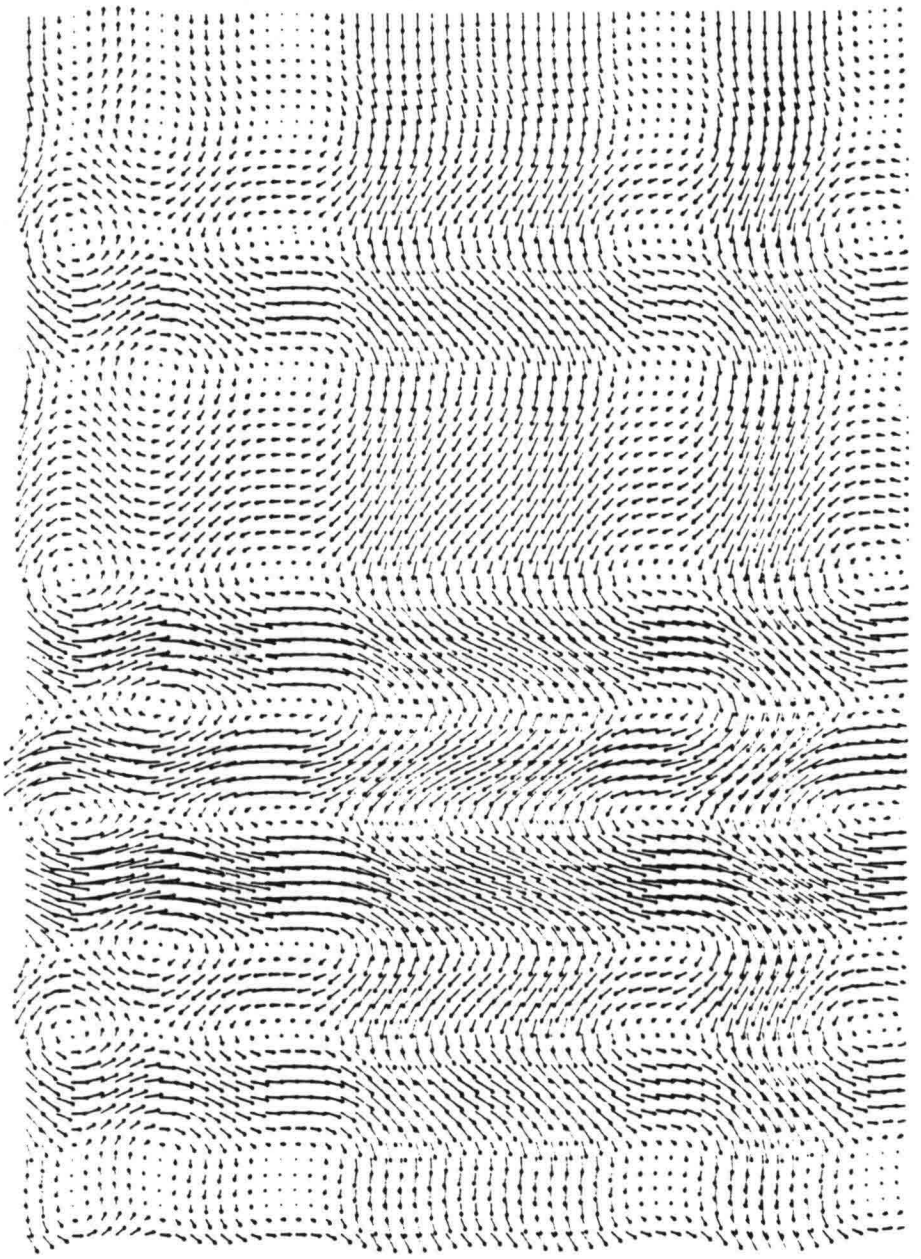

Figure 5 Particular "order" in velocity field if all components are defined on the same pair of axes (x,y)

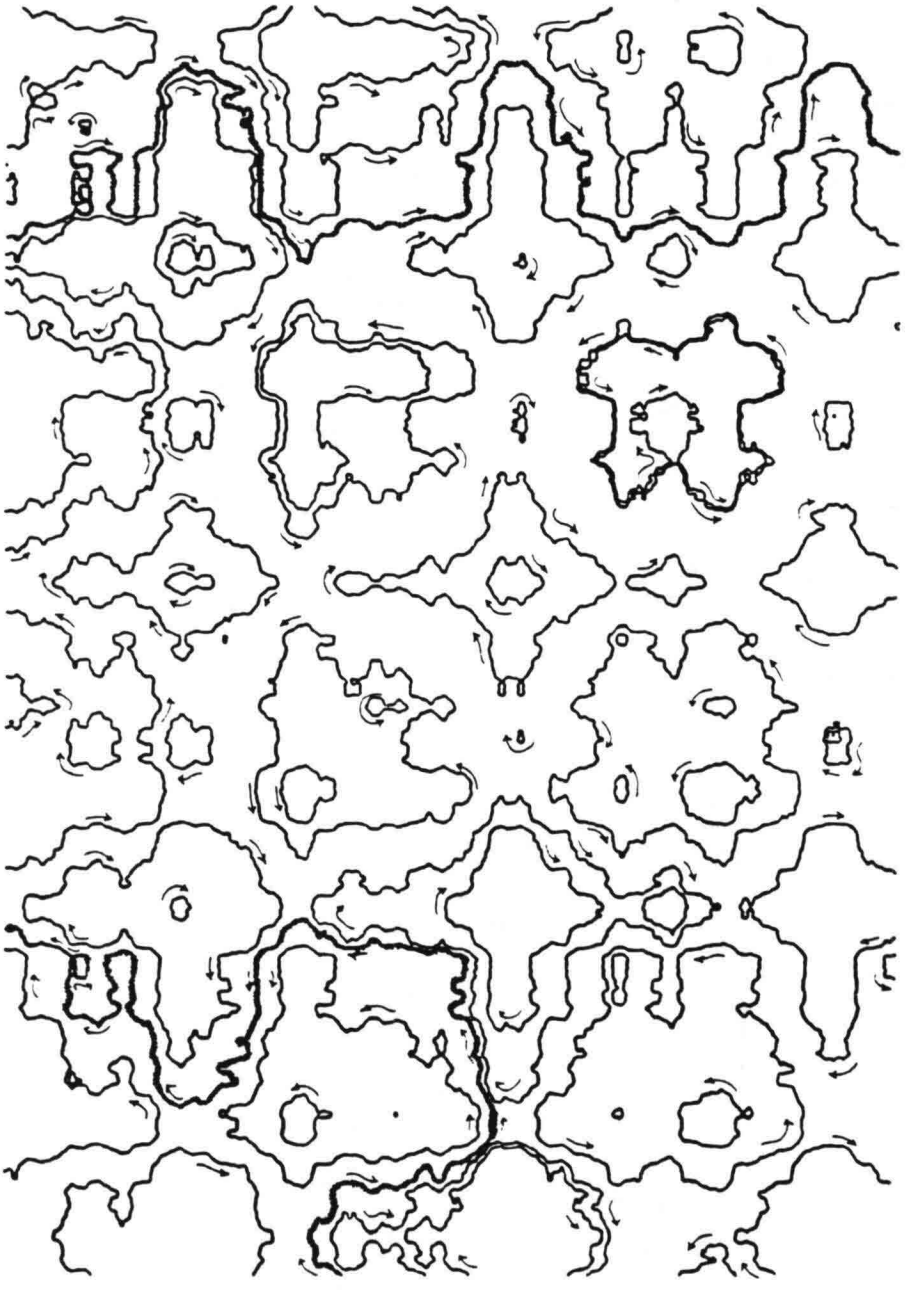

Figure 6 If all components are defined on the same pair of axes (x,y), this is reflected by a certain order in a set of particle tracks (stationary field)

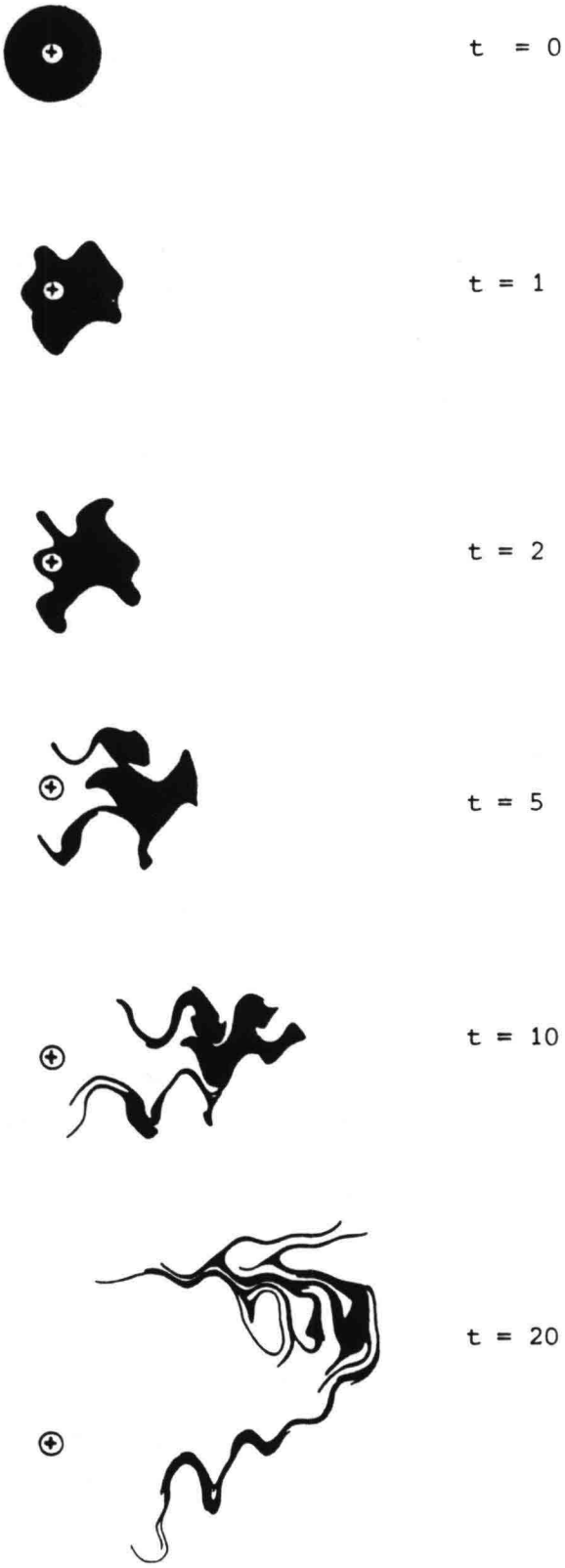

Figure 7

Advection of fluid blob $< \lambda_{max}$ in a stationary field

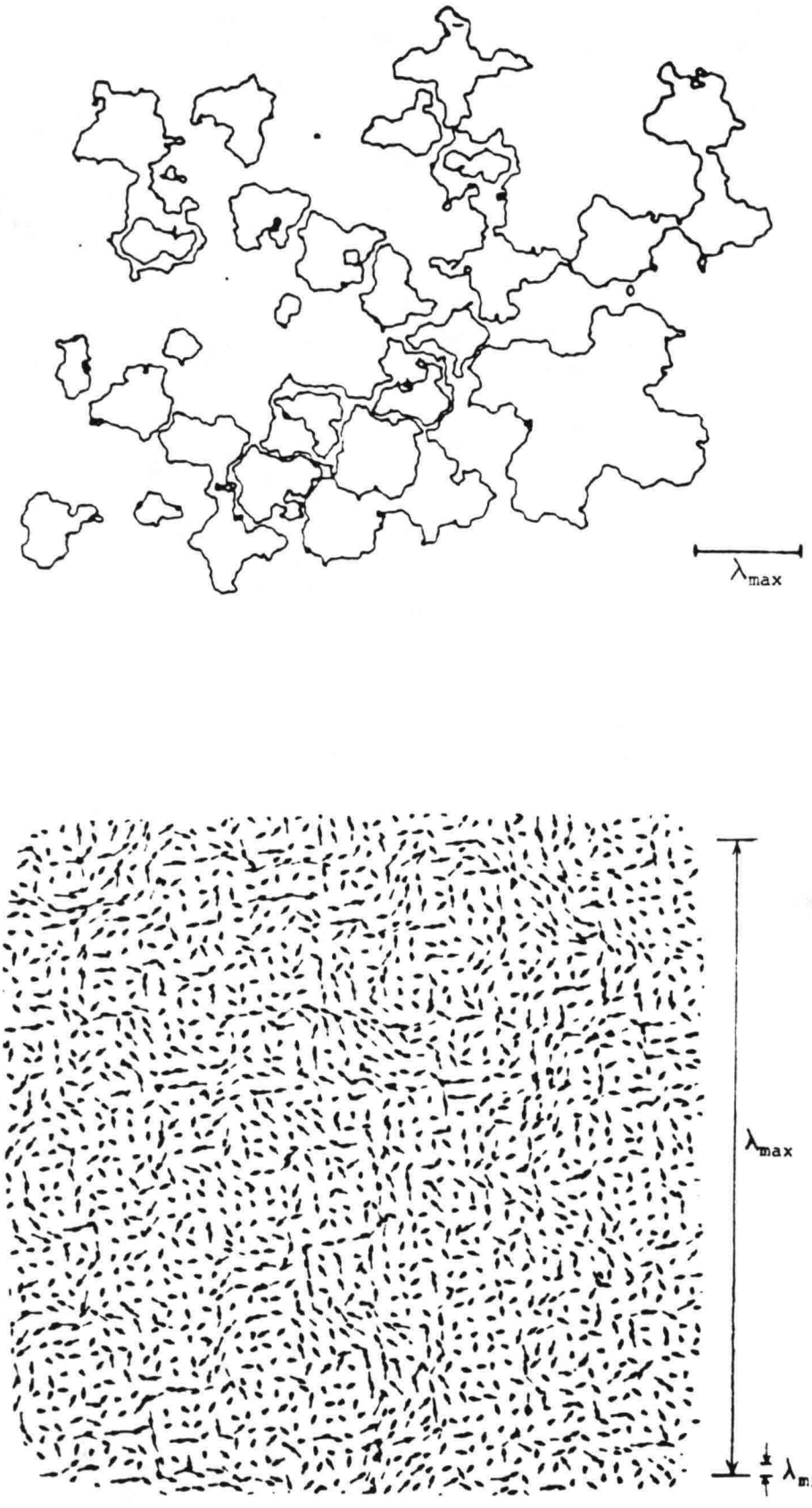

Figure 8 Particle tracks and velocity vectors with random direction of axes for each pair of modes (stationary field)

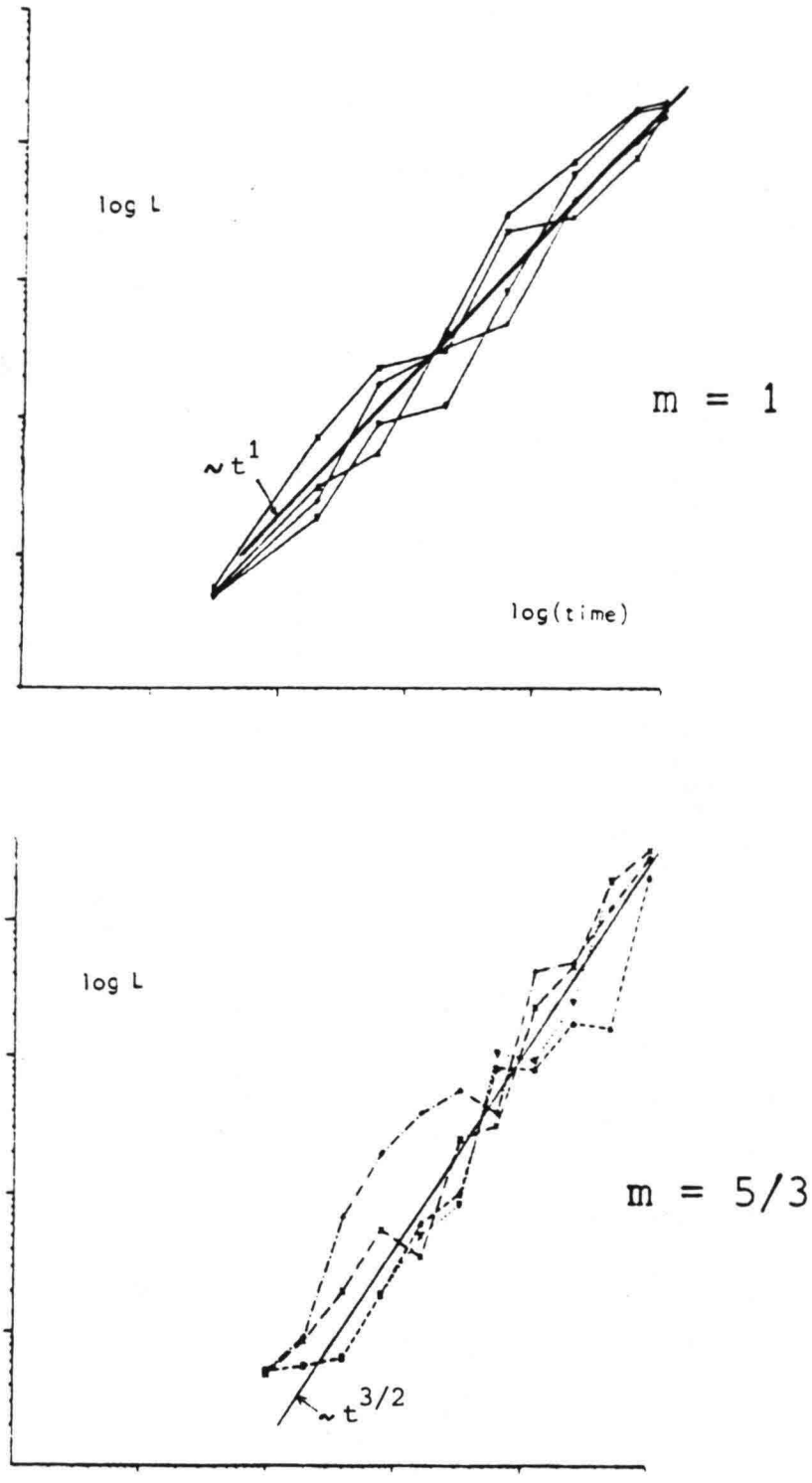

Figure 9

Patch growth L(t) with energy spectra $\sim k^{-1}$ and $k^{-5/3}$

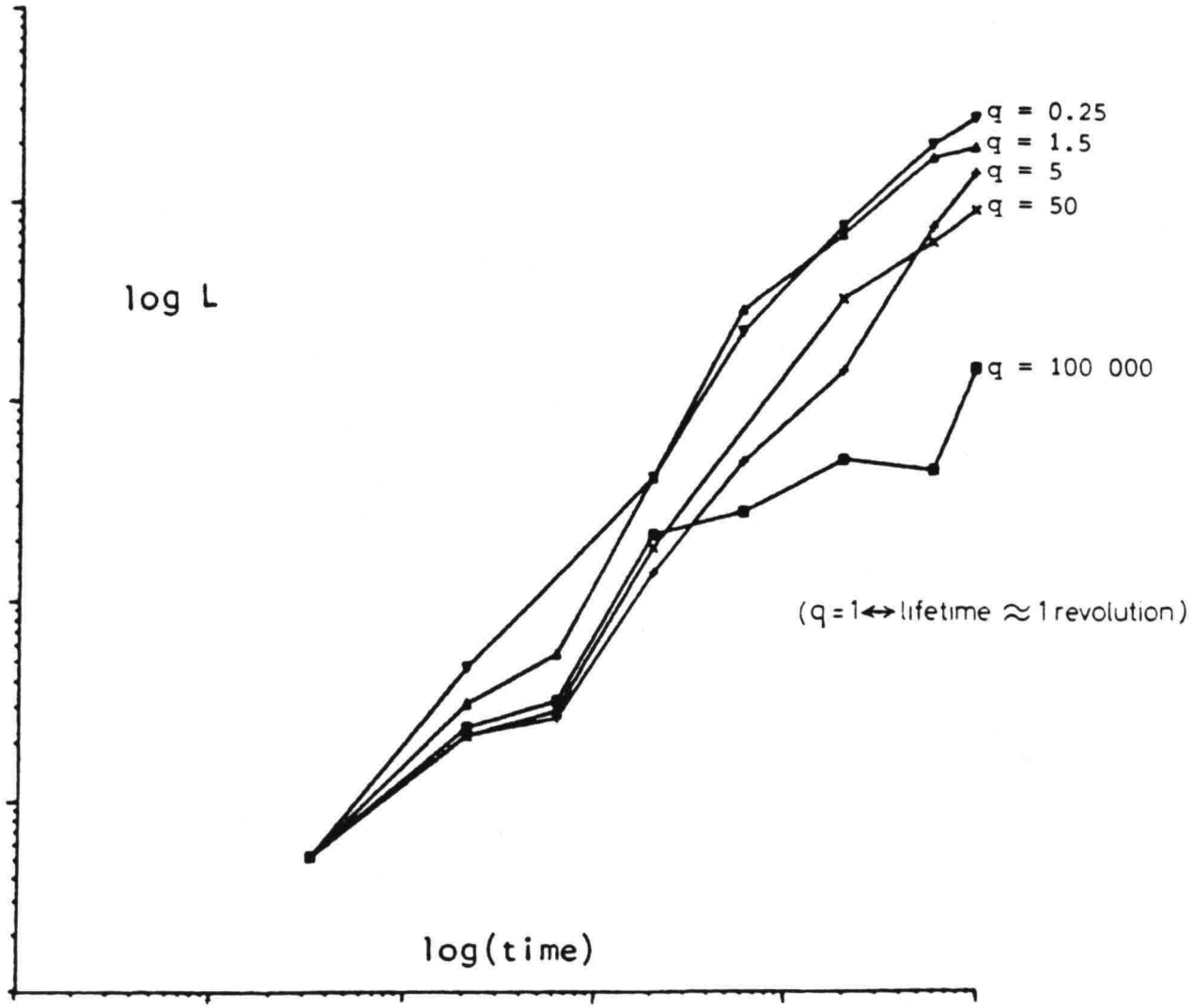

Figure 10 Patch growth in the range $\lambda_{min} \leqq L \leqq \lambda_{max}$ for various lifetimes of eddies

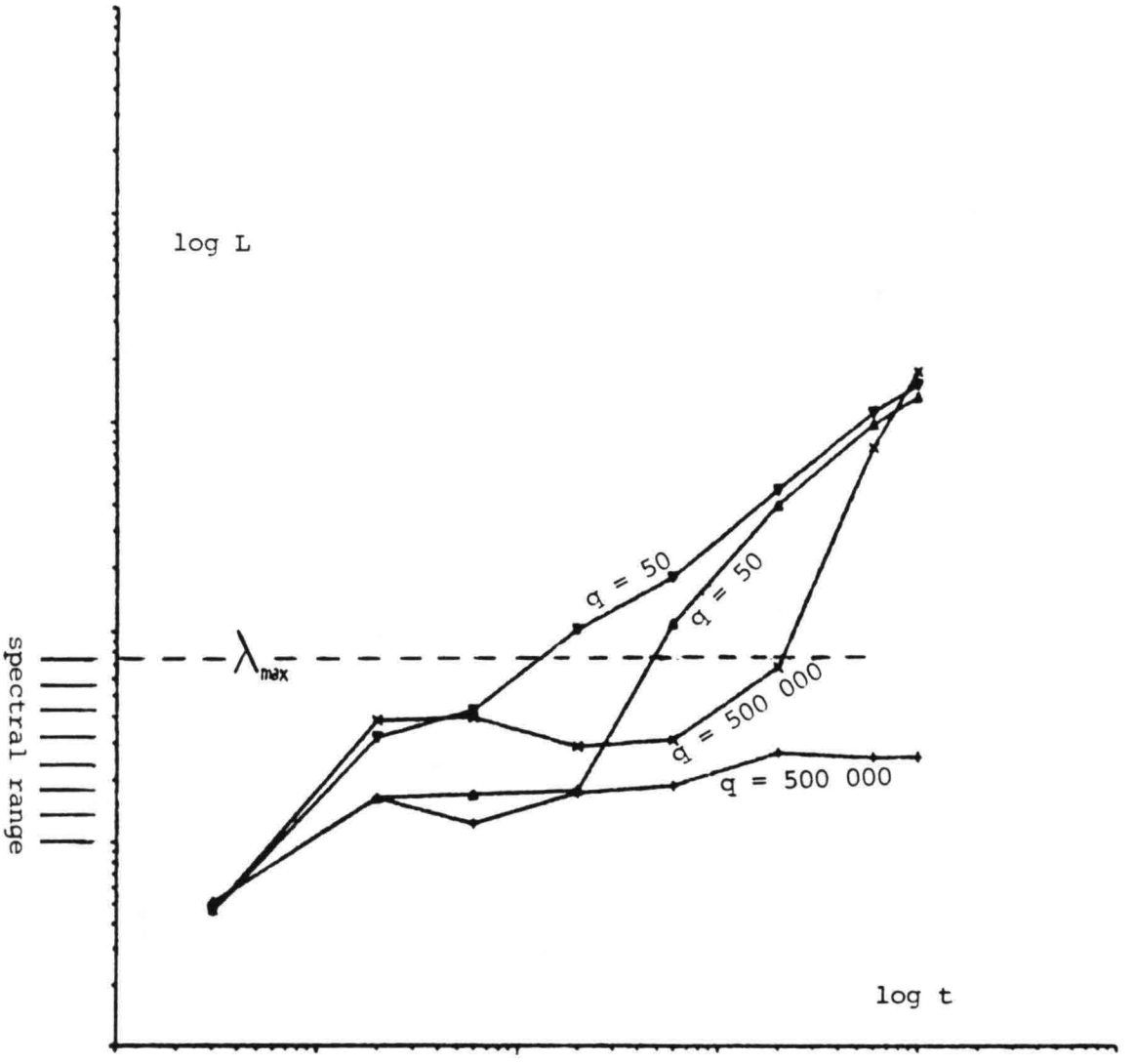

Figure 11 Patch growth beyond λ_{max} for various lifetimes of eddies

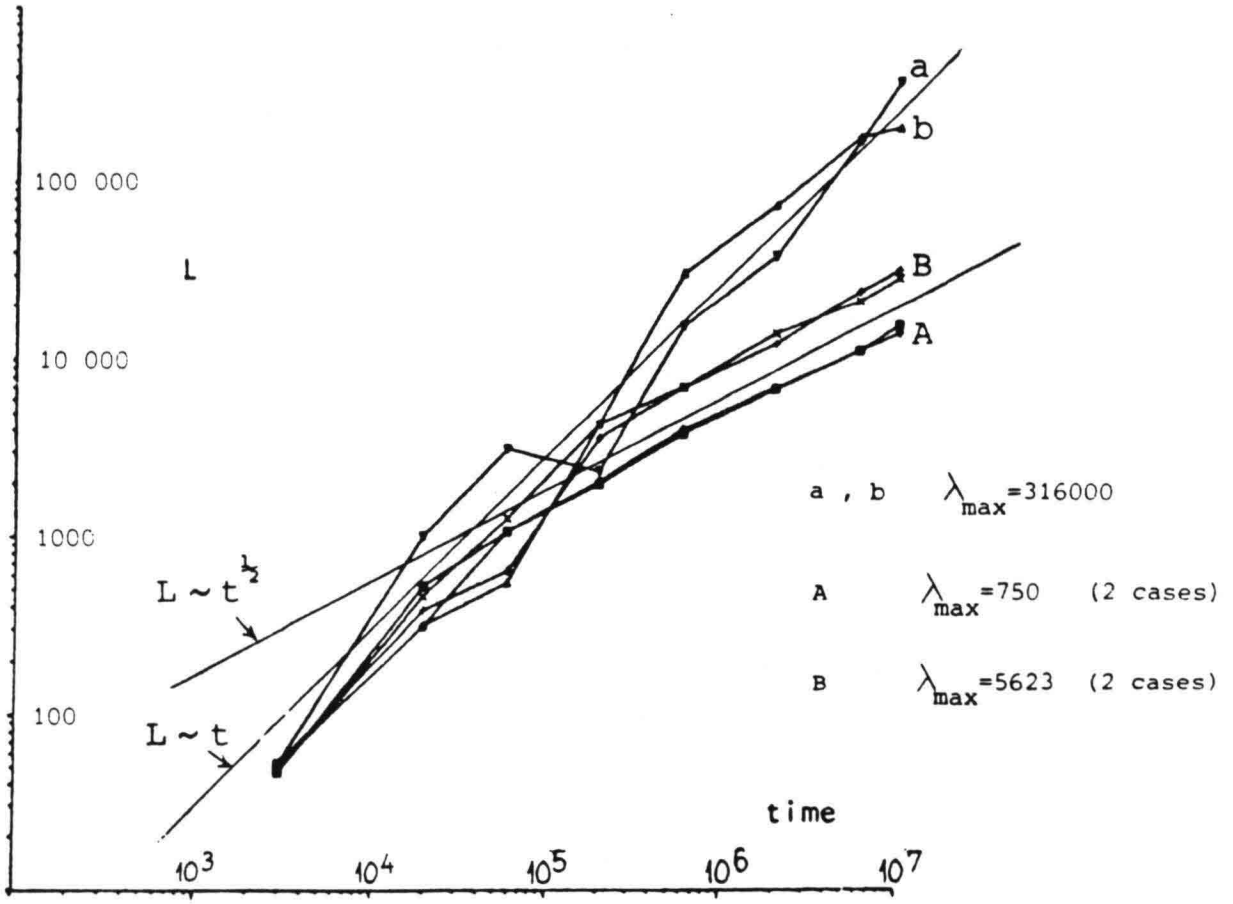

Figure 12 Patch growth (regular time dependent field) in ranges beyond λ_{max}

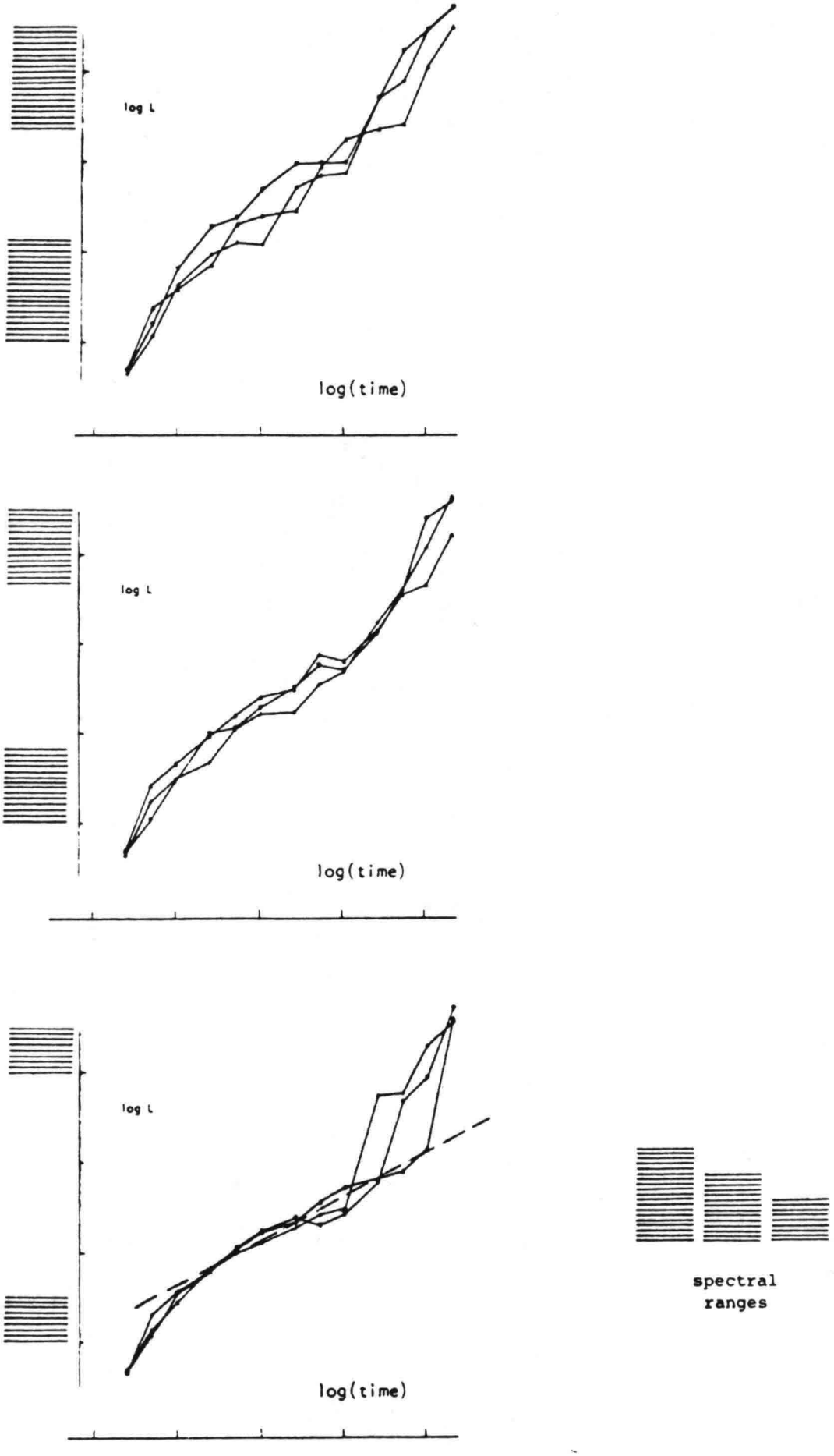

Figure 13 Patch growth within and around spectral gaps

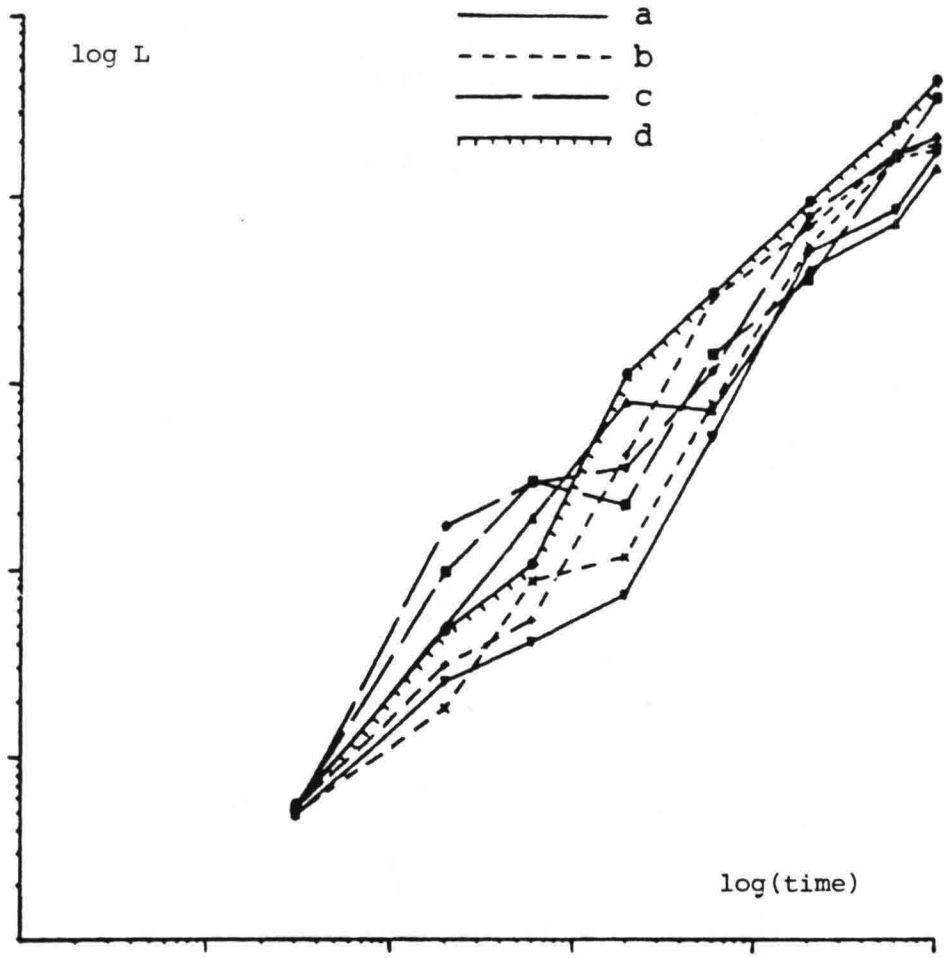

Figure 14 Patch growth in the range $\lambda_{min} \leqq L \leqq \lambda_{max}$ with various densities of spectral "lines" (wavelengths of spectral components).
a, b, c, d: 2, 4, 8 and 16 spectral components per (log.) decade respectively

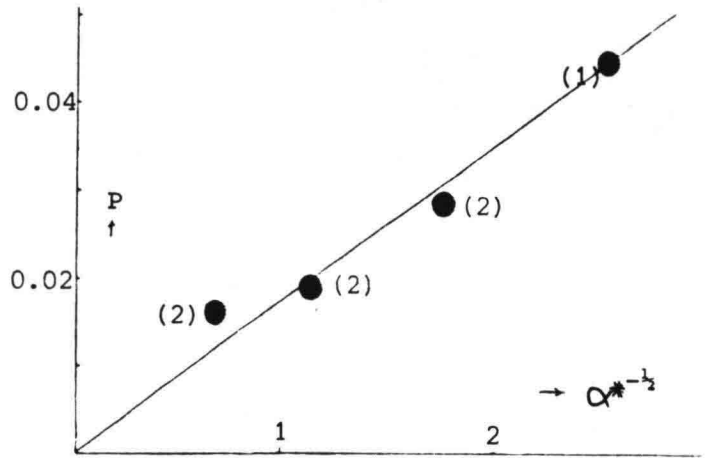

Figure 15 "Diffusion velocity" P as a function of spectral line density expressed as $\alpha^{*-1/2}$ (data set of figure 14); $\alpha^* = d\lambda/\lambda$

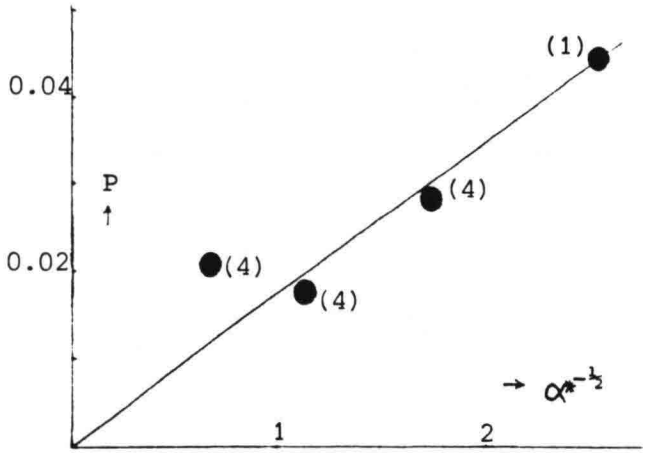

Figure 16 P as a function of $\alpha^{*-1/2}$ (extended data set)

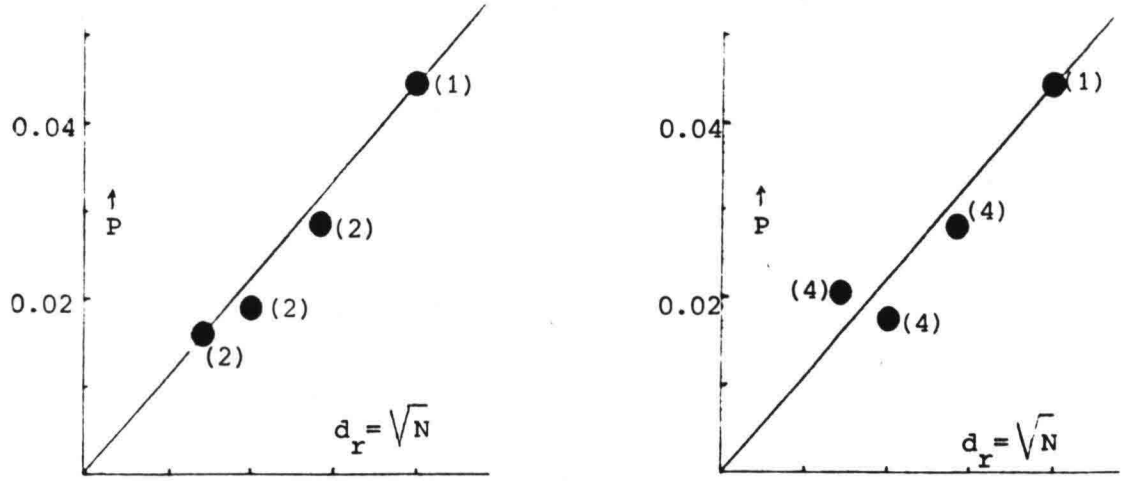

Figure 17 P as a function of the square root of the number of components per (logarithmic) decade

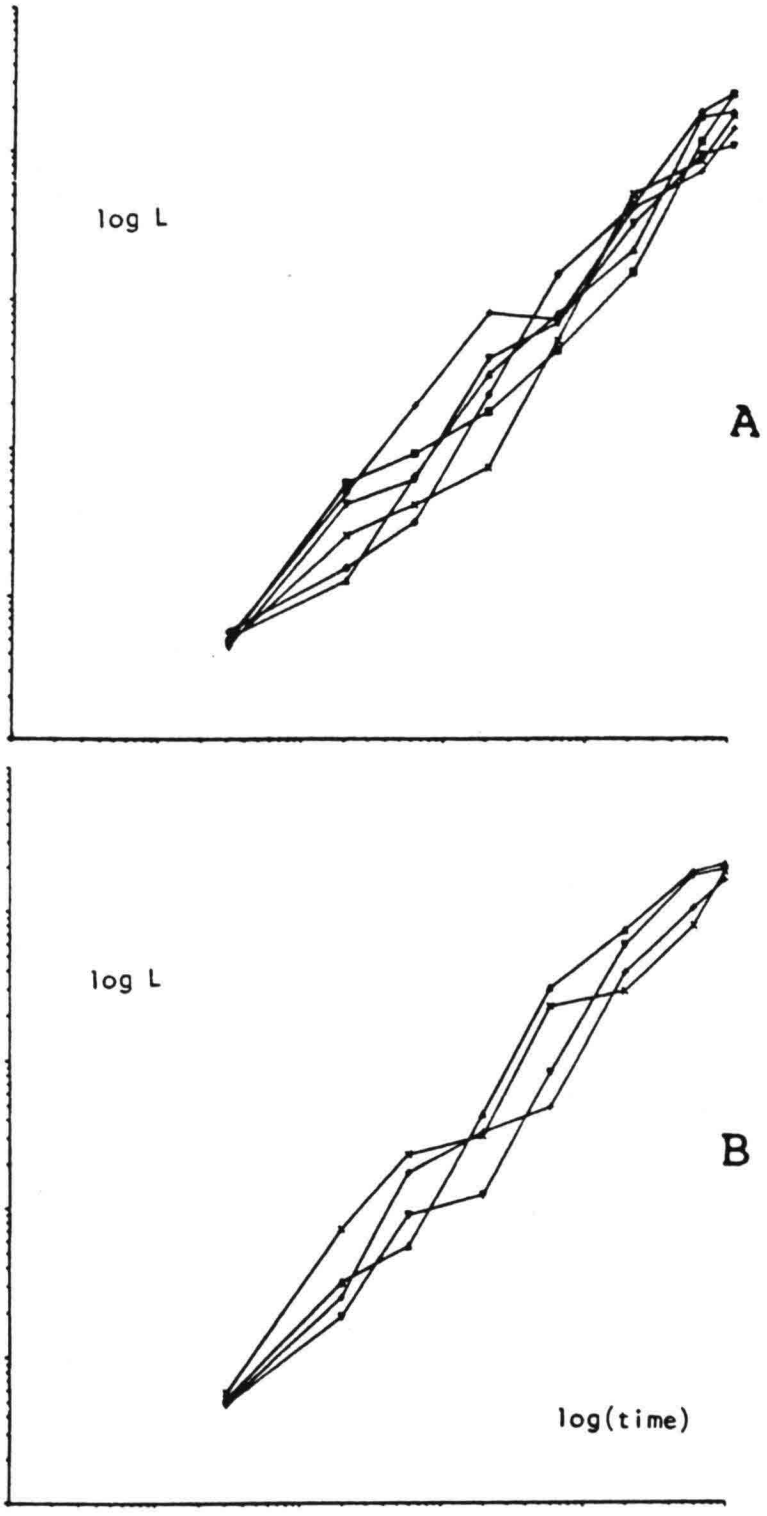

Figure 18 Variability of L(t)
A. two spectral components per decade
B. Four components per decade

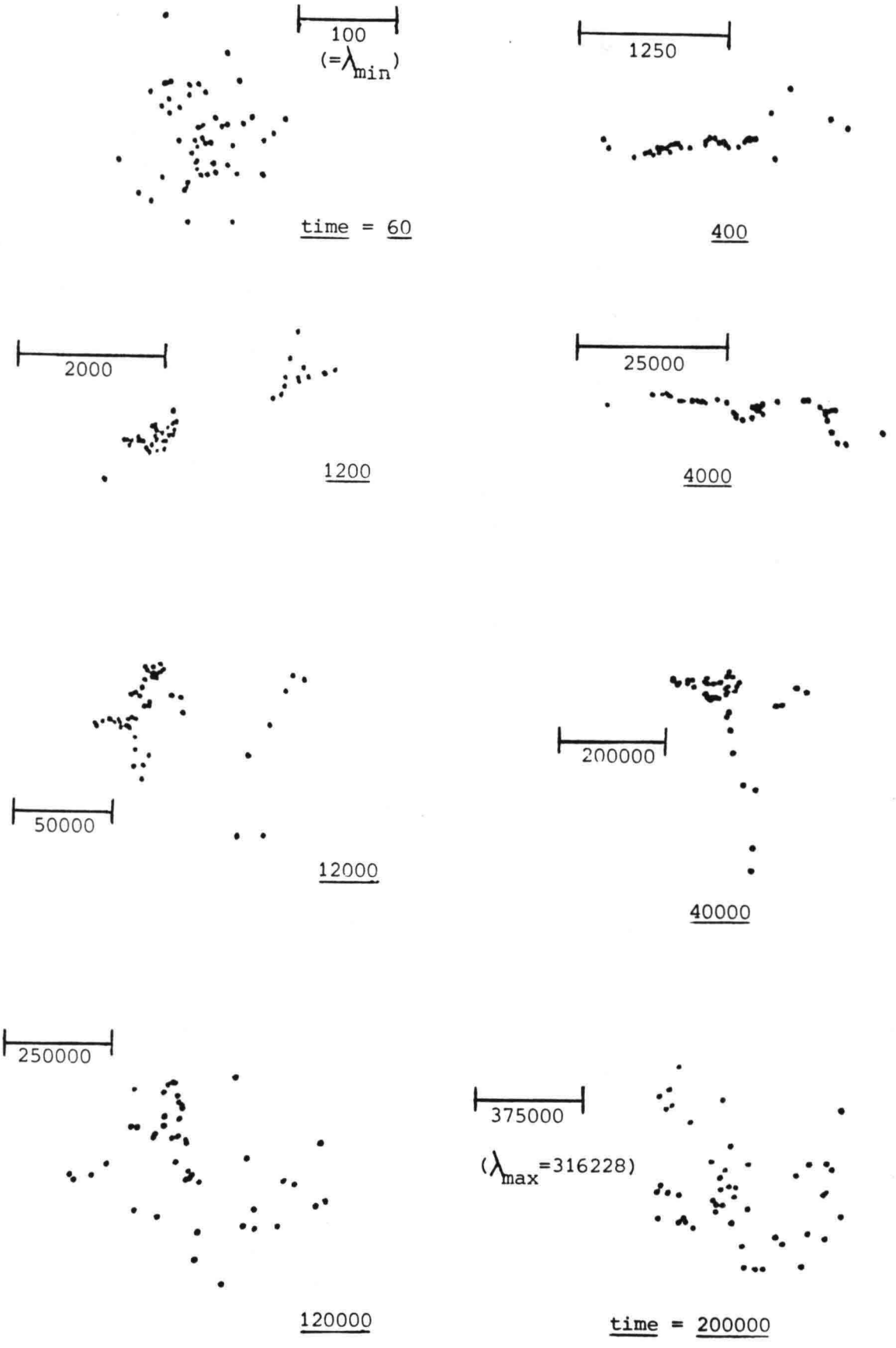

Figure 19

Patch shapes as a function of time

Scales and time
in arbitrary units

57 spectral components
3.5 decades (N=16)

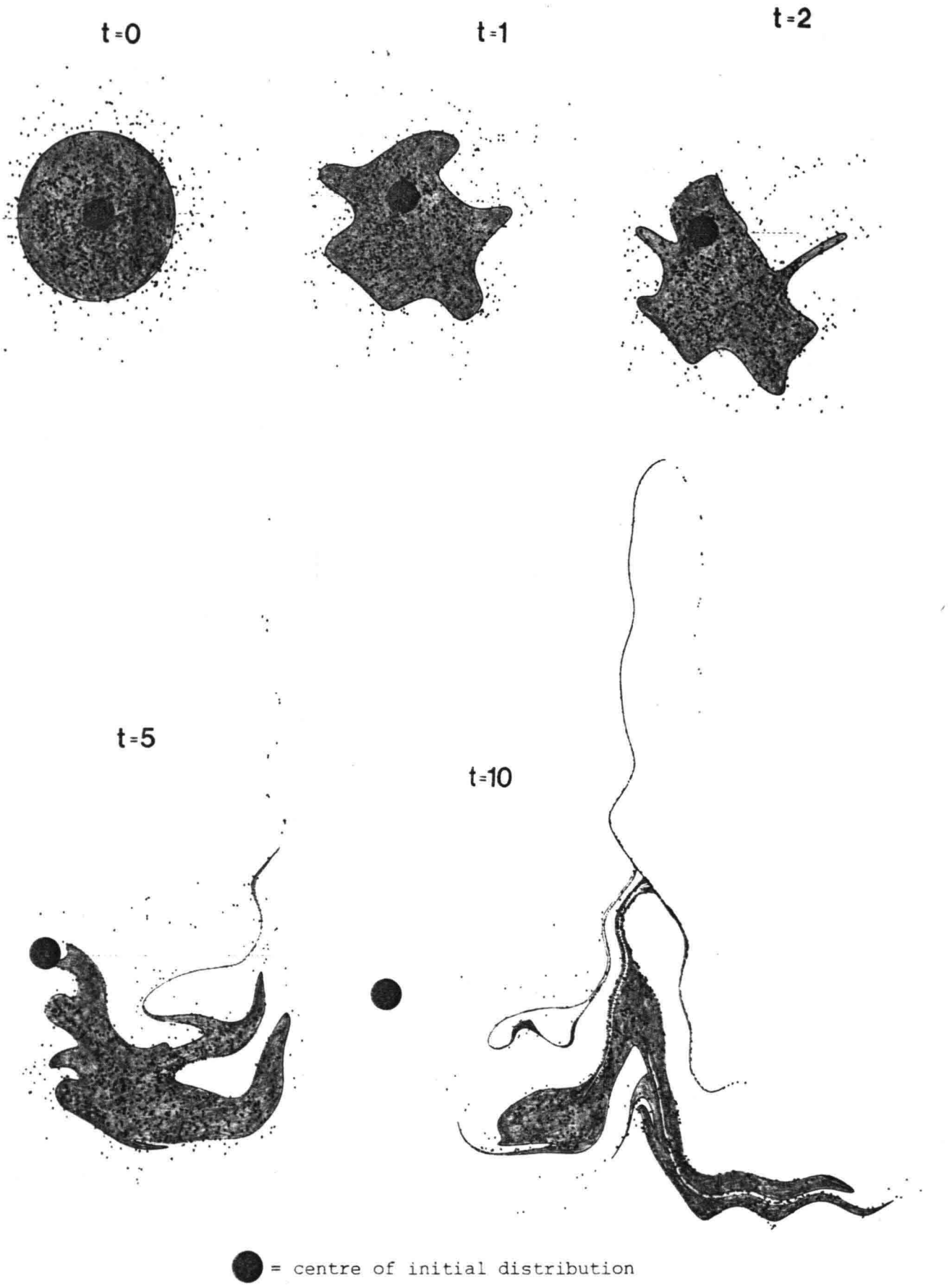

Figure 20 Relationship between the development of contours and particle clouds.

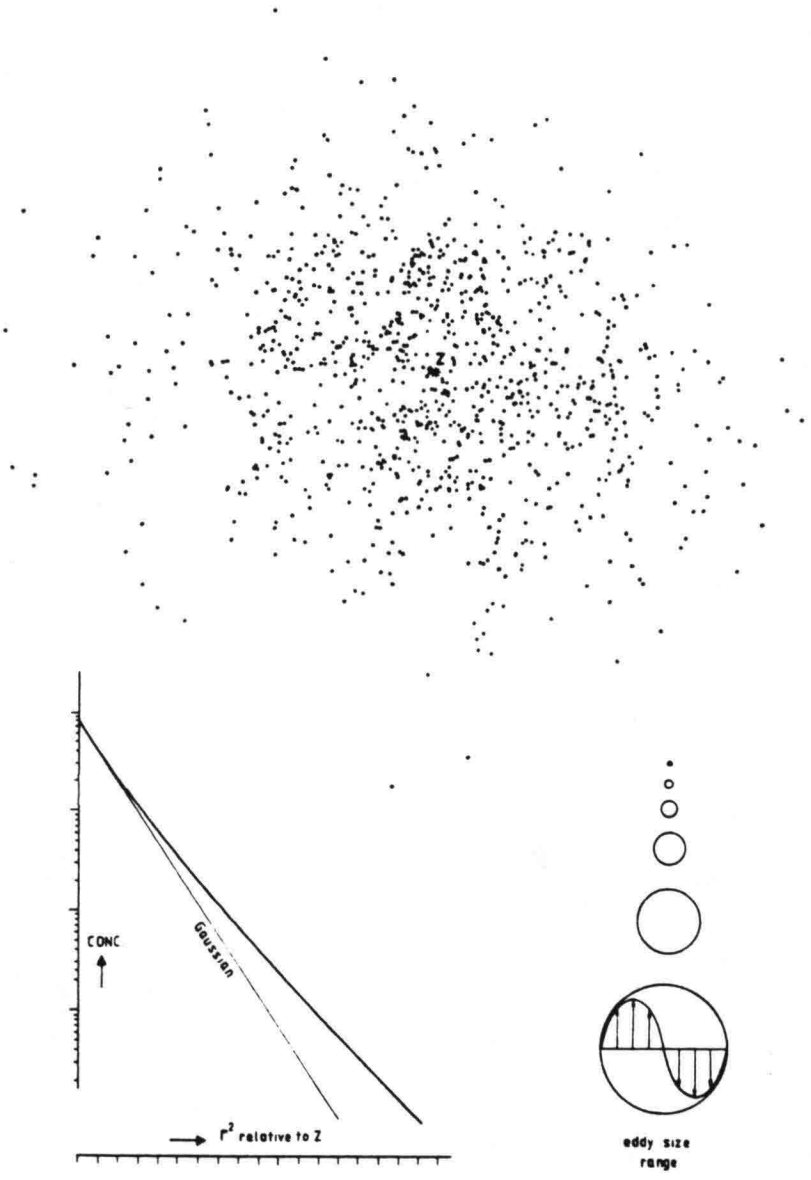

Figure 21 Distribution function of concentration as presented in VAN DAM, 1982 (1000 particles; 288 time steps)

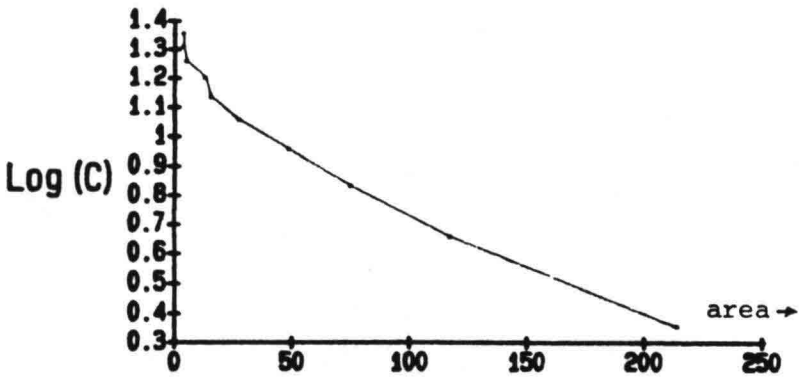

Figure 22 Example of distribution function (derived by other method than in figure 21) in a recent simulation (2000 particles)

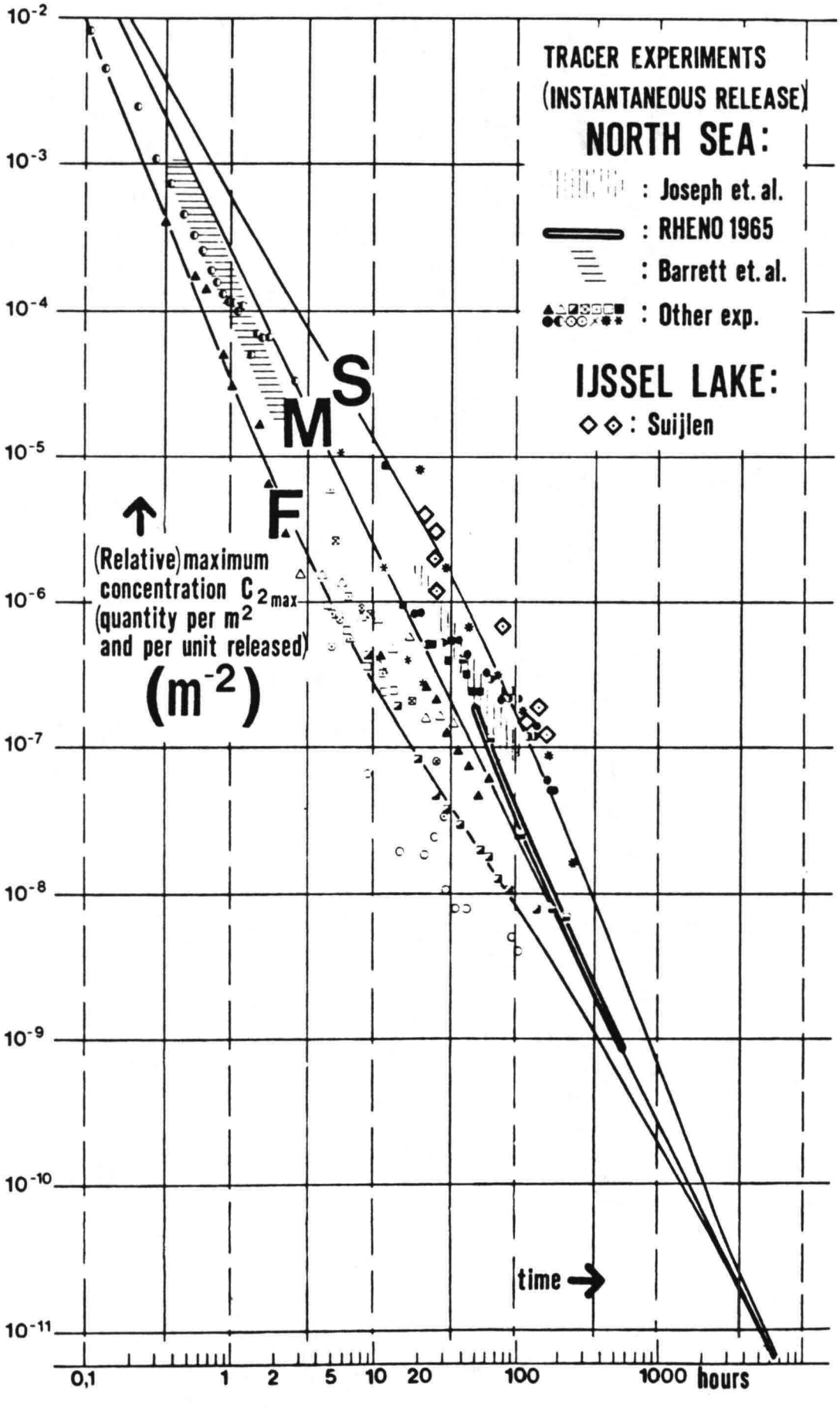

Figure 23 Results from instantaneous point release experiments in the North Sea (VAN DAM, 1980[a], 1982)
For comparison some results added from a region without tides (IJsselmeer, SUIJLEN, 1975)

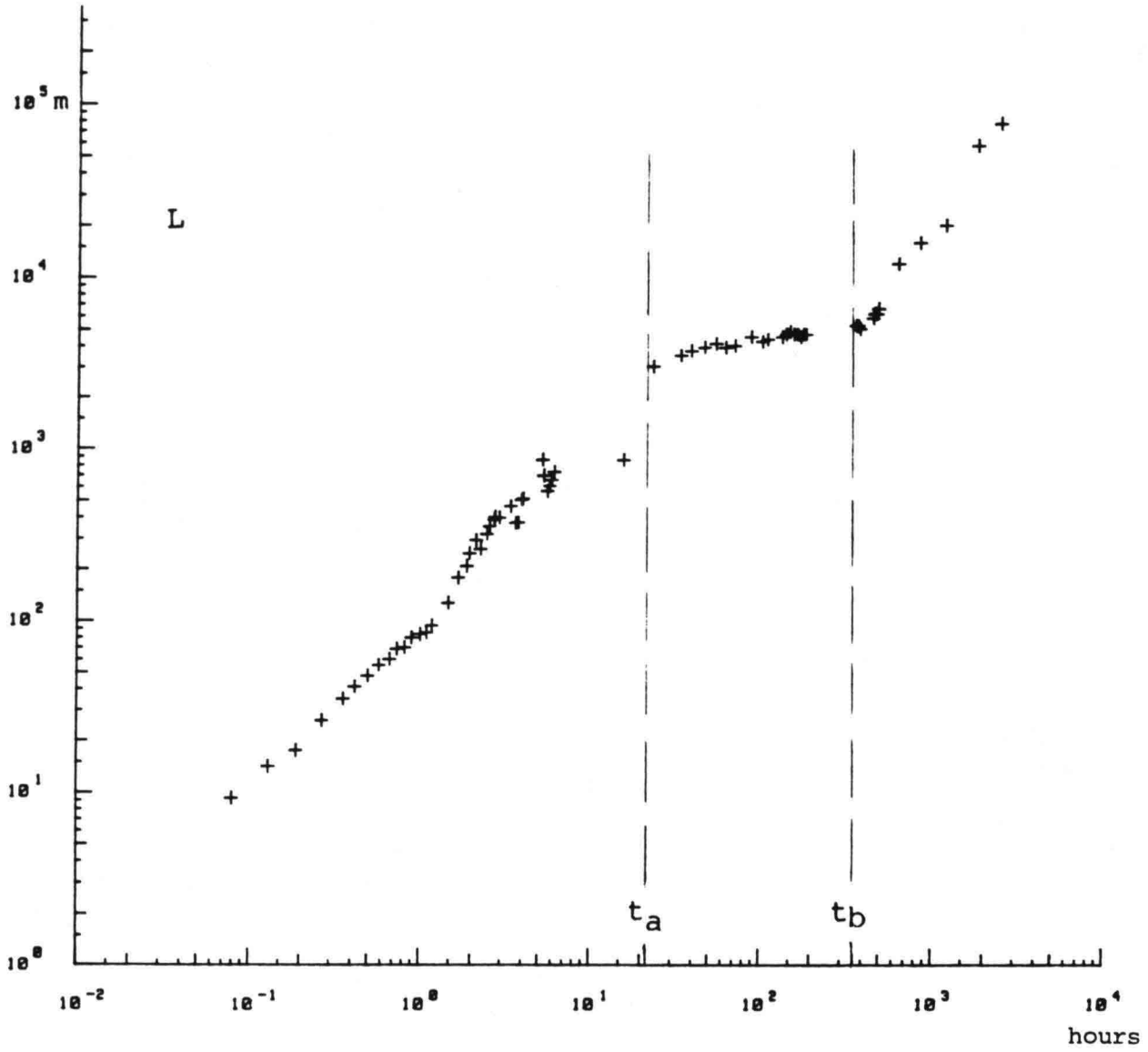

Figure 24 Example of apparent change in spectral conditions during a dye experiment on the North Sea (SUIJLEN et al., 1988)

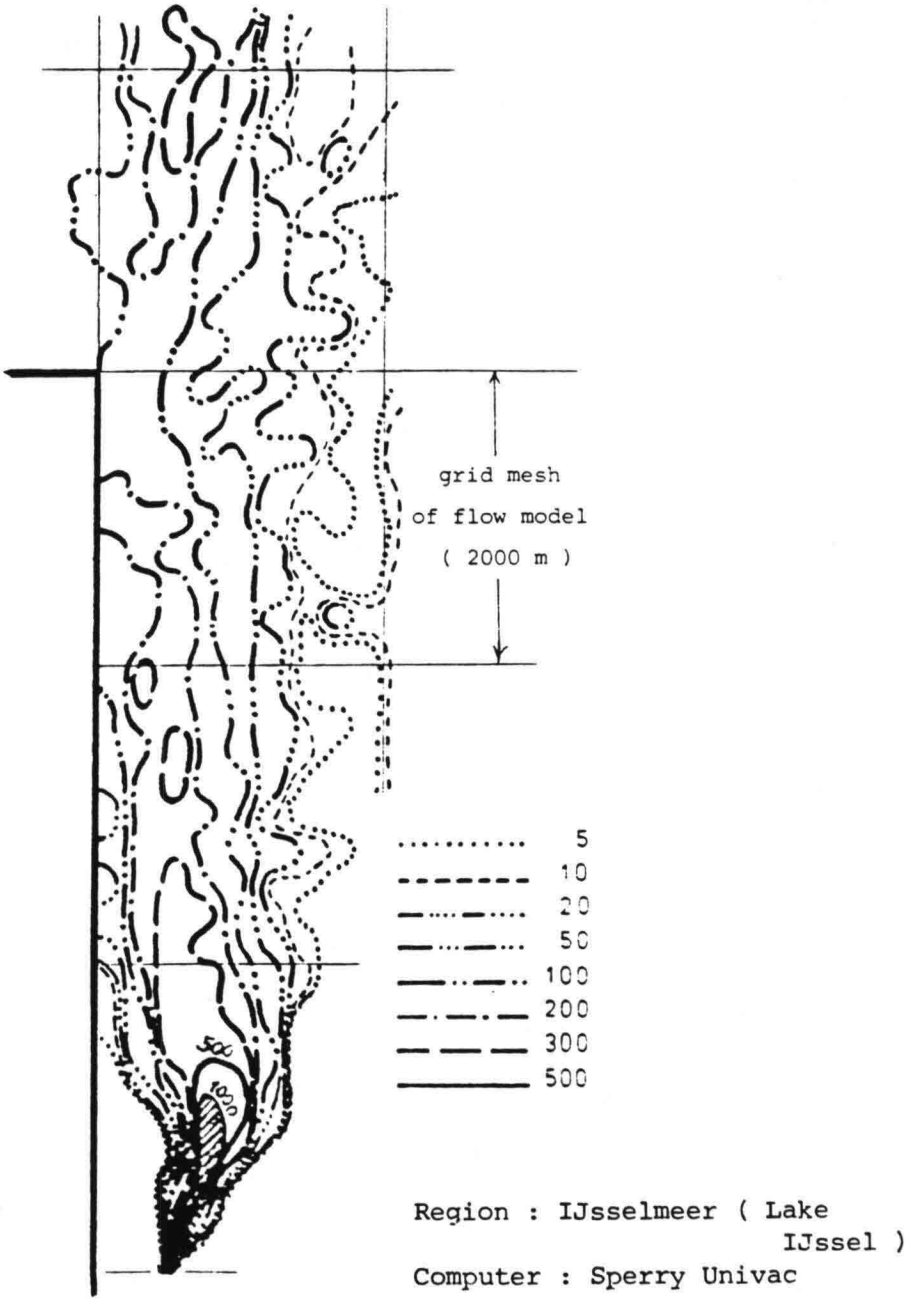

Figure 25 Example of a continuous release distribution computed by advecting discrete particles in velocity field from flow model, supplemented with (a small number of) additional spectral modes. From VAN DAM, 1985[e]